# Theory of Double-Layer Differential Capacitance in Electrolytes

J. Ross Macdonald and Carl A. Barlow, Jr.

*Texas Instruments Inc., Dallas 22, Texas*

(Received March 20, 1961)

A theory of the double layer in uni-univalent unadsorbed electrolytes is developed and used to analyze Grahame's experimental measurements of differential capacitance for NaF in water at 0° to 85°C and KF in methanol at 25°C. Excellent agreement with experiment is obtained except in the region of strong anodic polarization; this disagreement is tentatively ascribed to specific adsorption of anions, an effect not quantitatively considered in the present work. Although the quantities calculated herein relate to the entire double layer as, of course, do Grahame's data, the Gouy–Chapman theory of the diffuse part of the double layer (without dielectric saturation) is adequate in the present situation for all concentrations considered and has been used throughout. Consequently, the degree of agreement between theory and experiment found reflects primarily upon the applicability of the present theory of the inner layer. In the absence of specific adsorption this region is taken to be a hexagonally close-packed charge-free monolayer of solvent, physically adsorbed on the mercury electrode by dipole image forces. Adsorption anisotropy can lead to some dielectric saturation in the inner layer even at the electrocapillary maximum, the point of zero electrode charge. Neglecting association in the monolayer, the inner-layer dielectric constant and its dielectric saturation properties are calculated under three situations—where dipole image contributions are neglected, where the monolayer dipoles are imaged in the mercury electrode only, and where they are additionally imaged in an equipotential plane on the other side of the layer. The last case leads to an infinite set of images and to infinite series which are summed. These treatments all lead to much smaller dielectric constants and saturation constants than are found for bulk solvent. Comparison with values of these constants obtained from fitting the theory to the experimental data using a digital computer yields reasonably close agreement. New equations for the dependence of inner-layer thickness, volume, and dielectric constant on pressure and electric field, are derived and applied. The electrostatic pressure in this region is shown to consist of a capacitor-plate compressive term and an electrostrictive term, the latter originating only from the distortional and not the orientational polarization of the inner layer. As with the dielectric properties, the compressibility of the inner region found from curve fitting is of the right order of magnitude for both water and methanol solvents. The hump which occurs in water at low temperatures and small anodic polarization is attributed to the interplay of specific adsorption and dielectric saturation. Finally, it is pointed out that the usual method of separation of the inner-layer capacitance from the total differential capacitance by assuming the former to be in series with the diffuse-layer capacitance is unjustified in regions of appreciable specific adsorption, where the inner layer is no longer charge free.

## INTRODUCTION

In 1954, one of the present authors published a theoretical treatment of the double layer in unadsorbed electrolytes[1] and analyzed the NaF differential capacitance measurements of Grahame[2] for cathodic polarization at 25°C on the basis of this theory.[1] This work (hereafter referred to as I) was the first attempt to analyze the behavior of the inner, or charge-free, region of the double layer in terms of its averaged properties. Since 1954, several inadequacies of the earlier theory have become apparent; Grahame[3] has obtained considerable further data on NaF for a range of temperatures extending from 0° to 85°C, and a digital computer for convenient fitting of theory to experiment has become available. Therefore, the time seemed ripe to present an improved version of the early work at the American Chemical Society Symposium in Commemoration of David C. Grahame.[4] The present paper represents a final and more complete version of the work presented at this symposium.

The double layer with which we shall be concerned is assumed, in the absence of specific adsorption, to consist of the following parts. First, there is a space-charge region in the metallic electrode[5–10] analogous to the usual diffuse double layer of electrolyte theory. The effective thickness of this layer is so small for a good conductor such as mercury that its effect within the metal may be almost completely neglected. Next follows the inner, charge-free layer between the electrode and the electrolyte. Finally comes the diffuse double layer, made up of positive and negative ions and extending into the bulk of the electrolyte.

The basic equations of the simple diffuse double layer were first given by Gouy,[11] Chapman,[12] Fowler,[13] and Müller.[14] Independent derivations are found in the papers of Macdonald and Brachman[15] and of Gold.[16] The final results have been given in two different mathematical forms, the equivalence of which has not

[1] J. R. Macdonald, J. Chem. Phys. **22,** 1857 (1954).
[2] D. C. Grahame, J. Am. Chem. Soc. **76,** 4819 (1954).
[3] D. C. Grahame, J. Am. Chem. Soc. **79,** 2093 (1957).
[4] J. R. Macdonald, Symposium in Commemoration of David C. Grahame, 138th Meeting of the American Chemical Society, New York, New York, September 14, 1960. Abstracts of papers, p. 14-I.
[5] J. Bardeen, Phys. Rev. **49,** 653 (1936).
[6] H. Y. Fan, Phys. Rev. **62,** 388 (1942).
[7] C. Herring and M. H. Nichols, Revs. Modern Phys. **21,** 185 (1949). The work to 1948 is reviewed in this article.
[8] K. Huang and G. Wyllie, Proc. Phys. Soc. (London) **A62,** 180 (1949).
[9] R. Stratton, Phil. Mag. **44,** 1236 (1953).
[10] R. Furth and E. Morris, Proc. Phys. Soc. (London) **73,** 869 (1959).
[11] G. Gouy, J. Physique **9,** 457 (1910).
[12] D. L. Chapman, Phil. Mag. **25,** 475 (1913).
[13] R. H. Fowler, *Statistical Mechanics* (Cambridge University Press, London, England, 1929), 1st ed., pp. 282–283.
[14] H. Müller, Cold Spring Harbor Symposium Quant. Biol. **1,** 1 (1933).
[15] J. R. Macdonald and M. K. Brachman, J. Chem. Phys. **22,** 1314 (1954).
[16] L. Gold, J. Elect. and Control **5,** 427 (1958).

always been recognized.[17] Some of the deficiencies of simple diffuse double-layer theory for high ionic concentrations recently have been re-examined[18] and improved treatments of the problem[19,20] have been given. The results of this newer work are not needed in the present paper because except for regions of low ionic concentrations and low potential difference across the diffuse layer, where the simple theory is quite adequate, the inner layer dominates the capacitance of the series combination.

Grahame's differential capacitance results were obtained with a dropping mercury electrode. Since a very fine capillary tube was used for the mercury, it may be considered a spherical drop during the measurement. We have therefore carried out appropriate parts of the theory for a double layer surrounding a conducting sphere rather than for the usual plane electrode. Some of the results may be pertinent to the problem of hydration around a single ion or colloid particle.[21] For the present problem, where the ratio of sphere radius to inner-layer thickness is greater than $10^5$, the spherical solution reduces to that of the plane.

As in I, we are concerned with a system which we will describe by its averaged macroscopic properties such as dielectric constant and compressibility.[22a] We discuss the capacitance relations in the double layer and consider the effects of dielectric saturation and compression in the inner layer. In addition, we also consider the influence of specific adsorption, electrostriction, and a possible "natural" electric field at the electrode, assumed perfectly polarizable.

## BASIC CAPACITANCE RELATIONS

As long as the inner layer remains charge free, the charge[23] $q$ on the mercury electrode must equal in magnitude the total space charge in the diffuse layer. The differential capacitance of the double layer $C_T$ is then $(C_1^{-1}+C_2^{-1})^{-1}$, where the differential capacitance of the inner layer $C_1$ and that of the diffuse layer[24] $C_2$ are in series. When the inner region is not charge free, a modification must be made in this equation which is discussed later. In the quantitative parts of the analysis which follows, we usually ignore specific adsorption. In addition, since the effect on $C_T$ of dielectric saturation by the applied field in the diffuse layer has been shown[25] to be small, it is also ignored.

In the absence of dielectric saturation, $C_2$ may be written[26,27] as the following function of the field $E_2$:

$$C_2=(\epsilon_2/4\pi L_D)[1+(\tfrac{1}{2}E_2^*)^2]^{\frac{1}{2}}=8.85417\times10^{-8}(\epsilon_2/L_D)\cdot[1+(\tfrac{1}{2}E_2^*)^2]^{\frac{1}{2}} \quad (\mu\text{f/cm}^2), \quad (1)$$

where $E_2^*\equiv(eL_D/kT)E_2$, $L_D$ is the Debye length,[22] and $\epsilon_2$ is the static dielectric constant in the bulk of the solution. Numerical values such as that in (1) have been calculated from values of the fundamental constants given in references 28 and 29.

We shall need the potential drop $V_2$ across the diffuse layer, taking the far bulk of the solution to be at zero potential. [This choice of the reference potential is equivalent to referring all potentials to the electrocapillary maximum (ecm) potential.] We may write $V_2$ in terms of $E_2$ to give,

$$|V_2|=(2kT/e)\ln\{|\tfrac{1}{2}E_2^*|+[1+(\tfrac{1}{2}E_2^*)^2]^{\frac{1}{2}}\}=1.7234\times10^{-4}T\ln\{|\tfrac{1}{2}E_2^*|+[1+(\tfrac{1}{2}E_2^*)^2]^{\frac{1}{2}}\} \quad (\text{v}). \quad (2)$$

Since it is likely that the charge-free region is made up of a single monolayer of solvent, hexagonally closed packed on the electrode, we shall describe this layer by the following averaged properties: thickness $d$, static dielectric constant $\epsilon_1$, differential dielectric constant $\kappa_1$, compressibility $\beta$, and Poisson's ratio $\sigma$. In the absence of adsorption, $D_1=\epsilon_1E_1=4\pi q$ is constant and, as will be shown, $\epsilon_1$ is not proportional to $E_1^{-1}$; therefore, $\epsilon_1$ and $E_1$ must be separately constant throughout the inner layer.[30] Then, $V_1=E_1d$, where $d$ may depend upon $E_1$ if the layer is compressible. The total potential drop across the double layer is $V_0\equiv V_1+V_2$.

The boundary condition at the interface between the charge-free region and the diffuse layer is $E_2=\epsilon_1E_1/\epsilon_2$, giving $E_2$, and hence $C_2$ and $V_2$, in terms of $E_1$. In calculating $C_1$, account must be taken of possible variation of inner layer thickness with electric field. Let us take $d_0$ to be the thickness for $E_1=0$ and define the

[17] B. Breyer, Revs. Pure and Appl. Chem. **6,** 249 (1956).
[18] H. S. Frank and P. T. Thompson, J. Chem. Phys. **31,** 1086 (1959).
[19] M. J. Sparnaay, Rec. trav. chim. **77,** 872 (1958).
[20] H. Brodowsky and H. Strehlow, Z. Electrochem. **63,** 262 (1959).
[21] Work in progress by the present authors.
[22] Superscript letters refer to material supplementary to this article which has been deposited with the ADI Auxiliary Publications Project, Photoduplication Service, Library of Congress, Washington 25, D. C. A copy may be secured by citing the Document number. Advance payment is required. Make checks or money orders payable to: Chief, Photoduplication Service, Library of Congress. Document number and prices may be obtained from the authors at the by-line address.
[23] For convenience, quantities referred to as charge and capacitance will be understood to mean charge and capacitance per unit area where pertinent.
[24] A subscript 1 will be used when necessary to denote quantities defined in or pertaining to the inner layer, while a subscript 2 will be employed for diffuse layer quantities. For parameters such as electric field which vary with distance in the diffuse layer, the 2 designates the value in the diffuse layer at the boundary with the inner layer. Unless explicitly indicated, all reference to capacitance means differential not integral or static capacitance.
[25] D. C. Grahame, J. Chem. Phys. **18,** 903 (1950).
[26] D. C. Grahame, Chem. Revs. **41,** 441 (1947).
[27] J. R. Macdonald, J. Chem. Phys. **22,** 1317 (1954).
[28] E. R. Cohen, J. W. M. DuMond, T. W. Layton, and J. S. Rollett, Revs. Modern Phys. **27,** 363 (1955).
[29] J. A. Bearden and J. S. Thomsen, Am. J. Phys. **27,** 569 (1959).
[30] Compare with N. F. Mott and R. J. Watts-Tobin, Electrochim Acta **4,** 79 (1961). We are grateful to these authors for the chance to see advance copies of this manuscript, which treats much the same problem here considered but from a discrete-charge point of view and includes some treatment of specific adsorption.

normalized thickness $t \equiv d/d_0$. Then,

$$C_1 = dq/dV_1 = (dq/dE_1)(dE_1/dV_1), \quad (3)$$

where $dq/dE_1$, which involves the differential dielectric constant $\kappa_1$, is evaluated later. Since $V_1 = E_1 d = E_1 d_0 t$, one finally obtains

$$C_1 = (1/d_0)(dq/dE_1)\left\{t\left[1+\frac{d(\ln t)}{d(\ln|E_1|)}\right]\right\}^{-1}. \quad (4)$$

Note that $dq/dE_1$ and $t$ will both depend on $E_1$ when the layer exhibits dielectric saturation and compression. The rest of the paper is largely concerned with the form and results of such dependence.

## INNER-LAYER THICKNESS

Double-layer differential capacitance measurements near the ecm potential ($V_0 \cong 0$) do not yield the thickness of the charge-free layer but only the ratio $(\epsilon_1^0/d_0)$.[31] The value of this quantity at the point of minimum dielectric saturation (not necessarily the ecm, see later discussion) is approximately $3.4\times10^8$, derived from Grahame's data[3] on NaF–water at 25°C. Following Müller,[14] we consider the inner layer to be monomolecular. Therefore, we expect it to be hexagonally close packed in a plane and to have properties quite different from bulk solvent.[22b,32–36] In particular, a very thin layer of solvent will have a smaller than bulk dielectric constant[34,37] because of decreased molecular association and the near equality of the local and applied electric fields.[38] Such a lowered dielectric constant thus need not arise from saturation by a large natural field as discussed by Grahame[3,39] and one of the present authors.[40]

Based upon the best available experimental evidence,[41,42] we shall use the value of 3 A for the diameter of a water molecule in a close-packed monolayer. DeBoer[43] has mentioned that the radius of a surface atom is often included in estimating the distance between the surface and an adsorbed atom or molecule. We should probably include an ionic radius in estimating the thickness of the inner layer. Pauling gives the values 1.44,[44] 0.95,[45] 1.33,[45] and 1.36 A[45] for the radii of atomic Hg, $Na^+$, $K^+$, and $F^-$, respectively. Allowing for close packing and using somewhat less than the full Hg radius, we shall take 4.4 A for $d_0$ for NaF in water, of which 1.4 A is accounted for by atom and ion contributions.[22c] This leads to a value of $\epsilon_1^0$ of 14.9 for the average dielectric constant of the inner layer at 25°C, in agreement with the value of 15 found in I. For KF in methanol, a corresponding value of 5.4 A will be used. Since the fit found between theory and experiment is not strongly influenced by the value of $d_0$ used, an independent value of $\epsilon_1^0$ is needed to determine $d_0$ from differential capacitance measurements.

## DIELECTRIC CONSTANT AND ADSORPTION

A good review of the structure and dielectric constant of ordinary bulk water and electrolytes has been given by Robinson and Stokes.[46] As shown by Hasted, Ritson, and Collie[47] and Harris and O'Konski,[48] the dielectric constant of an electrolyte solution is reduced because of saturation by the ionic fields as the concentration is increased. We shall use this correction in the present work, the effect being to improve slightly the agreement with experiment near the ecm.

In the inner region $\epsilon_1$ will be made up of a distortion polarization contribution $\epsilon_\infty$ and an orientational contribution. Taking association in the inner region to be small and $E$ as the local field acting on the molecules, we may write for sufficiently small $E$

$$\epsilon_1 = \epsilon_\infty + 4\pi N_h[\langle \mu_v(E)\rangle/E] \quad (5)$$

$$\equiv \epsilon_\infty + ah(E), \quad (5')$$

where $\mu_v$ is the molecular vacuum dipole moment and $N_h$ is the dipolar concentration in the inner region.

The latest and seemingly most accurate determinations of $\epsilon_\infty$ for water[49] and methanol[50–52] yield 6.0 and about 4 to 6, respectively. We shall adopt the value of 6.0 for water; curve fitting seems to be facilitated by a value of 4.5 for methanol although the results are not very sensitive to the value chosen. $N_h$ cannot be calculated accurately but based upon hexagonal close packing of 3 A diameter spheres in an effective thickness of 4.4 A, $N_h = 2.92\times10^{22}$ cm$^{-3}$, the value we shall use.

The second term in Eq. (5) is the dipolar contribution and tends to zero as $E^{-1}$ in sufficiently high fields that dipole motion is inhibited. The pointed brackets in (5)

[31] J. R. Macdonald, J. Chem. Phys. **22,** 763 (1954).
[32] W. G. Eversole and P. H. Lahr, J. Chem. Phys. **9,** 530 (1941).
[33] J. C. Henniker, Revs. Modern Phys. **21,** 322 (1949).
[34] L. S. Palmer, A. Cunliffe, and J. M. Hough, Nature **170,** 796 (1952).
[35] T. Hori, Teion Kagaku, Butsuri Hen **15,** 34 (1956). U. S. Army Snow Ice and Permafrost Research Establishment, Translation No. 62, February 1960.
[36] O. Stern, Z. Electrochem. **30,** 508 (1924).
[37] C. G. Malmberg and A. A. Maryott, J. Research Natl. Bur. Standards **56,** 1 (1956).
[38] C. J. F. Böttcher, *Theory of Electric Polarization* (Elsevier Publishing Company, Amsterdam, 1952), p. 174.
[39] D. C. Grahame, Z. Electrochem. **59,** 740 (1955).
[40] J. R. Macdonald, J. Chem. Phys. **25,** 364 (1956).
[41] N. E. Dorsey, *Properties of Ordinary Water Substance* (Reinhold Publishing Corporation, New York, 1940), pp. 43–44.
[42] G. W. Brady and W. J. Romanow, J. Chem. Phys. **32,** 306 (1960).
[43] J. H. DeBoer, Advances in Catalysis **8,** 24, 334 (1956).
[44] L. Pauling, *The Nature of the Chemical Bond* (Cornell University Press, Ithaca, New York, 1960), 3rd ed., p. 256.
[45] Reference 44, p. 514.
[46] R. A. Robinson and R. H. Stokes, *Electrolyte Solutions* (Academic Press Inc., New York, 1959), pp. 1–23.
[47] J. B. Hasted, D. M. Ritson, and C. H. Collie, J. Chem. Phys. **16,** 1 (1948).
[48] F. E. Harris and C. T. O'Konski, J. Phys. Chem. **61,** 310 (1957).
[49] R. W. Rampola, R. C. Miller, and C. P. Smyth, J. Chem. Phys. **30,** 566 (1959).
[50] J. Ph. Poley, Appl. Sci. Research **B4,** 337 (1955).
[51] J. A. Saxton, Proc. Roy. Soc. (London) **A213,** 473 (1952).
[52] E. H. Grant, Proc. Phys. Soc. (London) **B70,** 937 (1957).

indicate an average over spatial configurations, and we shall assume that all dipole orientations are possible. Watts-Tobin[53] has applied a two-state model to the present situation based on the consideration that if the water forms strong bonds with the mercury the possibilities of orientation will be constrained by the bonding. The extent of this effect is not certain. Perhaps a better treatment would consist of a compromise between the present one and that of Watts-Tobin. The saturation function $h(E)$ is so defined that $h(0)=1$; thus, the unsaturated dielectric constant $\epsilon_1^0$ is $\epsilon_\infty+a$, where $a$ is the maximum dipolar contribution.

The calculation of the dipole term in (5) requires $\langle\mu_v(E)\rangle$. If $\theta$ is the angle between an ideal dipole vector and the direction of the applied local field $E_1$, then quite generally

$$\langle\mu_v\rangle=\mu_v\langle\cos\theta\rangle = \frac{\mu_v\int_0^\pi \cos\theta\,\exp\{-[W(\theta)/kT]\}\,\sin\theta d\theta}{\int_0^\pi \exp\{-[W(\theta)/kT]\}\,\sin\theta d\theta}, \quad (6)$$

where $W(\theta)$ is the energy of orientation of the dipole. If we consider the mercury to be a smoothed continuum, the dipoles will be imaged therein and the result will be more complicated than the Langevin[54] function, which for small fields yields $\langle\mu_v\rangle=(\mu_v^2/3kT)E_1$. Classical or quantum mechanical treatment leads to the following expression for the interaction energy of a dipole and its image[22d,55]:

$$W_i=-\mu_v^2(a_1+a_2\cos^2\theta)/2S^3, \quad (7)$$

where $S$ is the dipole-image distance and $a_1=a_2=1$. If we consider the ions in the diffuse double layer to approximate another equipotential surface at the outer Helmholtz plane, the dipoles will also be imaged in this plane. The interaction energy now has the same form as (7) only now $a_1$ and $a_2$ are given by the following expressions:

$$\left.\begin{aligned} a_1&=\tfrac{1}{8}(\Sigma_2+\Sigma_3-2\Sigma_1),\\ a_2&=\tfrac{1}{8}(6\Sigma_1+\Sigma_2+\Sigma_3),\end{aligned}\right\} \quad (8)$$

where $S$ is the distance between the conducting (imaging) sheets, $a_3(\leq S/2)$ is the distance between the dipole centers and one of the sheets, and

$$\left.\begin{aligned} \Sigma_1&=\sum_{n=1}^{\infty} n^{-3}=1.2020569,\\ \Sigma_2&=\sum_{n=1}^{\infty}\frac{2n[n^2+3(a_3/S)^2]}{[n^2-(a_3/S)^2]},\\ \Sigma_3&=(S/a_3)^3.\end{aligned}\right\} \quad (9)$$

For the only case we are considering $a_3/S=0.5$ and $\Sigma_2=8.828793$, $\Sigma_3=8$, $a_1=1.8030849$, and $a^6=3.0051419$. Note that we have neglected the effects of molecular distortion and higher multipole moments.

Some of the neglected factors, as well as wave function overlap,[9,56-60] will tend to make the dipoles line up preferentially in one direction.[22e] We represent this effect by a "natural" field which combines all the above anisotropies into a single term. We arbitrarily choose the anisotropy energy to have the form

$$W_a=W_0[\sin^2(\tfrac{1}{2}\theta)-1]=-\tfrac{1}{2}W_0[1+\cos\theta], \quad (10)$$

where $W_0$ measures the strength of the anisotropy. Clearly $W_a$ must depend on $\theta$, and we have taken such dependence to have the highest possible symmetry consistent with the desired binding anisotropy. If $W_0<0$, as we find to be the case from the fitting of Grahame's data, then the tendency is for the negative poles of dipoles to point outward from the Hg.

Collecting all terms in the energy $W(\theta)$, including the effect of the external field, we find to within an additive constant,

$$W(\theta)=-[\mu_vE_1+\tfrac{1}{2}W_0]\cos\theta-(a_2\mu_v^2/2S^3)\cos^2\theta. \quad (11)$$

Now define $E\equiv E_1+E_0$, where $E_0\equiv W_0/2\mu_v$; $x\equiv\mu_vE/kT$, $y\equiv[a_2\mu_v^2/2kTS^3]^{\frac{1}{2}}$, and $z\equiv x/2y=E[S^3/2a_2kT]^{\frac{1}{2}}$. Note that the anisotropy energy constant $W_0$ is thus directly related to the previously mentioned natural field $E_0$. If $E_0$ is determined from curve fitting, $W_0$ can be evaluated. Using the above definitions, (6) becomes

$$\langle\mu_v\rangle=\mu_v\int_{-1}^{1}\gamma\exp(x\gamma+y^2\gamma^2)d\gamma\Big/\int_{-1}^{1}\exp(x\gamma+y^2\gamma^2)d\gamma \quad (12)$$

$$=\mu_v\left[-(z/y)+\frac{y^{-1}\sinh x}{e^xY(y+z)+e^{-x}Y(y-z)}\right],$$

where

$$Y(\xi)=\exp(-\xi^2)\int_0^\xi\exp(x^2)dx \quad (13)$$

is $\exp(-\xi^2)$ times Dawson's integral,[61] which is itself also proportional to erfi$(\xi)$. If image forces are ignored but the anisotropy energy is retained, one again obtains the Langevin function, now involving the effective field $E$ rather than $E_1$. At zero effective field,

[53] R. J. Watts-Tobin, Phil. Mag. **6**, 133 (1961).
[54] Reference 38, p. 161.
[55] J. Bardeen, Phys. Rev. **58**, 727 (1940).
[56] N. G. McCrum and J. C. Eisenstein, Phys. Rev. **99**, 1326 (1955).
[57] J. C. P. Mignolet, Discussions Faraday Soc. **7-8**, 105 (1949-50).
[58] R. V. Culver and F. C. Tompkins, Advances in Catalysis **11**, 73 (1959).
[59] J. C. P. Mignolet, *Chemisorption*, W. E. Garner, editor (Academic Press Inc., New York, 1957), pp. 118-120.
[60] J. C. P. Mignolet, Bull. soc. chim. Belges **64**, 126 (1955).
[61] H. G. Dawson, Proc. London Math. Soc. **29**, 519 (1897).

the unsaturated dipolar contribution to the dielectric constant is

$$\lim_{E\to 0}[\langle\mu_v\rangle/E]=(\mu_v^2/3kT)\left\{\frac{3[y-Y(y)]}{2y^2Y(y)}\right\}$$
$$\equiv(\mu_v^2/kT)\Delta_0, \qquad (14)$$

and the term in curly brackets represents the deviation from the simple Langevin function result. The quantity $\Delta_0\equiv[y-Y(y)]/[2y^2Y(y)]$ is just the value of $[\langle\cos\theta\rangle/x]$ as $E$ goes to zero. Although $Y(\xi)$ cannot be evaluated exactly in closed form, an excellent table of this function exists,[62] and it may be readily calculated with a digital computer, the course followed here. The results of such calculations will be summarized in the next section.[63]

It is unlikely that the entire binding energy of a water molecule physically adsorbed on the mercury electrode is made up of permanent-dipole image attraction and anisotropy energy. In addition, there will certainly be smaller induction and dispersion effects[64] arising from molecular polarizability, but these will be neglected here because of the larger effects associated with the large permanent dipoles. At any temperature, the average image binding energy with $E=0$ is, from (7),

$$\langle W_i\rangle=-\mu_v^2[a_1+a_2(\langle\cos^2\theta\rangle)_0]/2S^3$$
$$=-\mu_v^2[a_1+a_2\Delta_0]/2S^3. \qquad (15)$$

The average value of the anisotropy energy with no applied field is

$$\langle W_a\rangle=-\tfrac{1}{2}W_0(1+\langle\cos\theta\rangle), \qquad (16)$$

where $\langle\cos\theta\rangle$ must now be calculated from (12) using $\langle\cos\theta\rangle=\langle\mu_v\rangle/\mu_v$ and taking $E_1=0$. At absolute zero, these binding energies reach their maximum values which are

$$\left.\begin{aligned}\langle W_i\rangle&=-\mu_v^2[a_1+a_2]/2S^3,\\ \langle W_a\rangle&=-W_0.\end{aligned}\right\}T=0. \qquad (17)$$

Using $1.85\times10^{-18}$ esu for $\mu_v$ for water, $S=4.4$ A, and $E_0=-1.52\times10^6$ v/cm, a value determined later, one finds $(\langle W_i\rangle)_{\max}=-0.58$ kcal/mole for single image attraction, $-1.4$ kcal/mole for infinite images, and $(\langle W_a\rangle)_{\max}=-W_0=0.27$ kcal/mole. Note that at 0°K the presence of the anisotropy energy ensures that the dipoles will all be lined up with their positive poles next to the mercury surface. At 25°C, the anisotropy binding energy is about $0.3kT$. The above results are of reasonable orders of magnitude. In particular, it is gratifying that the anisotropy energy, determined in a completely different way from the image energy, is from two to five times smaller than the latter.[22f]

The "natural" field $E_0$ arising from the binding-energy anisotropy is not necessarily a real field but is only a quantity which has the effect of such a field as far as dipole orientation and dielectric saturation are concerned. Since $E_0$ leads to some saturation, even when the applied field $E_1$ is zero, we have defined $\epsilon_1(E)$ in Eq. (5) as $D/E(=D_1/E_1)$, where $E\equiv E_0+E_1$ and $D\equiv\epsilon_1E\equiv D_0+D_1$. At the ecm, the average charge on the electrode $q$ is zero, and we shall take the applied electric field zero also at this point. This assumption, which leads to nonzero dielectric saturation at the ecm, in apparent agreement with experiment, necessitates that the "natural" displacement $D_0$ not contribute to the average electrode charge, which, by Gauss's law, will then be given by $q=\epsilon_1E_1/4\pi$. Had Gauss' law been applied to $D$ rather than $D_1$, the ecm potential would have occurred at $E_1=-E_0$, a value for which there is no saturation.[22g]

## DIELECTRIC SATURATION

There has been a number of treatments of dielectric saturation for bulk material,[65–68] none of which can be directly applied to the present problem because each includes association and uses the internal field appropriate for bulk material. We expect to find that the results of the last section, expecially Eq. (12), give more realistic dependence of $\langle\mu_v\rangle$ in the present application. We shall now express the foregoing results in a simplified, one-parameter form.

From the definition of the differential dielectric

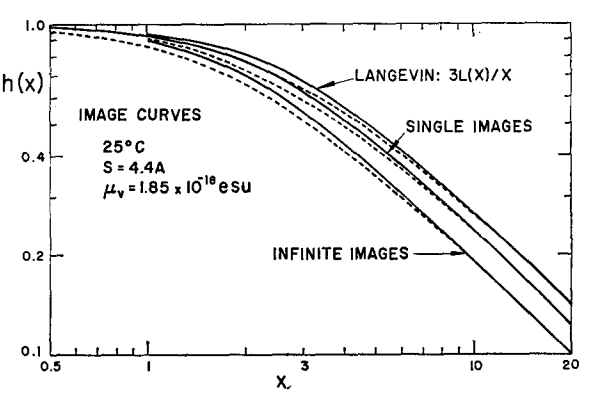


FIG. 1. Normalized dielectric saturation curves. Dash lines: Eq. (18), matching at high fields.

[62] B. Lohmander and S. Rittsten, Kgl. Fysiograf. Sällskap i Lund Förh. **28,** 45 (1958).

[63] In connection with a magnetic dipole problem, F. G. West [J. Appl. Phys. **32,** 249S (1961)] has independently obtained a result of the same form as Eq. (12).

[64] F. London, Trans. Faraday Soc. **33,** 8 (1937).

[65] Reference 38, pp. 193–198.

[66] F. Booth, J. Chem. Phys. **19,** 391, 1327, 1615 (1951); **23,** 453 (1955). Note that the 10% correction made in Eq. (3.12) of the last cited article has been applied incorrectly by the author.

[67] J. J. O'Dwyer, Proc. Phys. Soc. (London) **A64,** 73 (1951).

[68] J. A. Schellman, J. Chem. Phys. **26,** 1225 (1957). Using Schellman's value $g_2=5$, his equations lead to a considerably smaller dielectric saturation constant for water than Booth's or O'Dwyer's work predicts. Further, the value of 5 does not, seemingly, follow from Schellman's formula for $g_2$.

constant $\kappa \equiv dD/dE$ it follows that $\kappa = \epsilon + E(d\epsilon/dE) \equiv \epsilon_\infty + ag(E)$ and $g(E) = h(E) + E[dh(E)/dE]$. In agreement with Grahame,[69] we use the following explicit forms:

$$h(E) = (b^{\frac{1}{2}}E)^{-1} \tan^{-1}(b^{\frac{1}{2}}E), \tag{18}$$

$$g(E) = [1 + bE^2]^{-1}, \tag{19}$$

which are of the proper high-field limiting character. In these equations, $b$ is a constant controlling the strength of saturation effects.

For comparison with present results, it is desirable to obtain values of the saturation constant $b$ which best describe bulk water and methanol.[22h,66,70–74] For small saturation we may write

$$\epsilon^0 - \epsilon \cong \tfrac{1}{3}(\kappa^0 - \kappa) \cong E^2\delta, \tag{20}$$

and comparison with (18) or (19) yields for the conventional saturation parameter $\delta$,

$$\delta \cong \tfrac{1}{3}ab. \tag{21}$$

The present work leads to the following expressions for $a$ and $h(E)$:

$$a = 4\pi N_h \mu_v^2 \Delta_0 / kT, \tag{22}$$

$$h(E) = \left[ -(z/y) + \frac{y^{-1}\sinh x}{e^x Y(y+z) + e^{-x} Y(y-z)} \right] \Big/ X\Delta_0. \tag{23}$$

When image effects are omitted, one obtains,

$$a = 4\pi N_h \mu_v^2 / 3kT, \tag{24}$$

$$h(E) = (3/x)\, L(x) \equiv (3/x)\,(\coth x - x^{-1}), \tag{25}$$

where $L(x)$ is the Langevin function. The values of $b$ which make the high-field values of (18) equal to those of (23) and (25) are

$$b = (\pi x \Delta_0 / 2E)^2, \qquad \text{(images)} \tag{26}$$

$$b = (\pi x / 6E)^2. \qquad \text{(no images)} \tag{27}$$

These values will not lead to exactly the $\delta$ values which could be derived from (23) and (25) for the initial saturation range, but they apply better over the range of appreciable saturation important in the present work.

The forms of the saturation functions $h(x)$ are shown as solid curves in Fig. 1. The Langevin curve is a universal function of $x$, valid for any temperature. The two image curves, however, are calculated for 25°C. The dotted curves show the degree of fit possible using Eq. (18) together with the final-slope values of $b$ above. The maximum error, about 6%, is quite small enough for present purposes.

TABLE I. Comparison of inner-layer dielectric parameters at 25°C.

| Theory and assumptions | $a$ | $\nu$ | $r^2$ | $b \times 10^{14}$ (cm/v)$^2$ |
|---|---|---|---|---|
| Bulk water, experimental | 72.3 | 1.455 | 0.9998 | (12) |
| Onsager-Booth, bulk water, no association, $N$ | 22.4 | 1 | 1 | 1.8 |
| Langevin, $N_h$ Eqs. (24), (27) | 10.2 | 1 | 1 | 0.6 |
| Single images, $N_h$ Eqs. (22), (26) | 11.6 | 1.114 | 0.9998 | 0.8 |
| Infinite images, $N_h$ Eqs. (22), (26) | 14.6 | 1.300 | 0.9999 | 1.3 |
| Experimental, derived from present curve fitting | 8.9 | 2.15 | 0.9999 | 2.27 |

Table I shows some experimental results and the results of calculations using the preceding formulas. The values in the table apply to bulk water or water in the inner layer. A value of $\mu_v = 1.85 \times 10^{-18}$ esu has been used, together with $\epsilon_\infty = 6$ and $d_0 = S = 4.4$ A. It has been found that the temperature dependence of $a$ over the range of 0° to 100°C can be well expressed by an equation of the form $a(T) = HT^{-\nu}$, where $T$ is the absolute temperature and $H$ is a constant. Values of $\nu$ shown have been obtained from least-squares analysis of experimental data or theoretical results. Such fitting is first carried out using the linearized form of the above equation, here obtained by taking logarithms of both sides, which allows both $H$ and $\nu$ to be obtained. This procedure yields a correlation coefficient whose square will be later distinguished by a subscript $t$, denoting transformed. Using the resulting value of $\nu$, another least-squares analysis can be made considering $T^{-\nu}$ as the linear variable. The square of a correlation coefficient obtained in this way will be quoted throughout this work without a subscript, as in Table I.

The results given in the first row of Table I are based on the experimental results of Malmberg and Maryott[37] and of Malsch.[70] The results of the second row are included to show the theoretically expected values of $a$ and $b$ for bulk water (internal field not equal to external field) without association. The 10% correction developed by Booth[66] in his later work has been included in the calculation of $b$.

The next three rows of the table should be compared to the last row, where some of the later curve fitting results are presented. Agreement is good to order of magnitude. No closer agreement can be expected from the present approximate theoretical treatments; nevertheless, they justify our taking much smaller values of the maximum dipole contribution to the dielectric

[69] D. C. Grahame, J. Chem. Phys. **18**, 903 (1950).
[70] J. Malsch, Physik Z. **29**, 770 (1928); **30**, 837 (1929).
[71] W. F. Brown, Jr., *Handbuch der Physik*, edited by S. Flügge, (Springer-Verlag, Berlin, 1956), Vol. 17, p. 111.
[72] Reference 69, p. 905.
[73] J. A. Schellman, J. Chem. Phys. **24**, 912 (1956).
[74] D. C. Grahame, J. Chem. Phys. **21**, 1054 (1953). Grahame actually speaks of fitting our Eq. (19) to Booth's curve, but it is clear that in fact he used (18).

constant $a$ and the saturation constant $b$ than appropriate for bulk water. Of the many factors which mitigate against close agreement between theory and experiment here, especially important are probably the asphericity of the molecules in the inner layer, planar molecular interaction, the small distances involved, and the strong inhomogeneous image fields, which may lead to values of $\mu_v$ different from the vacuum value used here.

Disagreement between theory and experiment shows up especially in the temperature dependence results. None of the theoretical values of $\nu$ is close to the experimentally determined value of 2.15. This figure is itself suspiciously close to 2.0 and, in fact, it is found that least-squares analysis of the values of $a$ derived from the data using $\nu=2$ yields $r^2=0.9998$, almost as high as that with 2.15. Further, the earlier equations show that $b$ should have the same temperature dependence as $[a(T)]^2$, provided $N_h$ and $\mu_v$ are taken temperature independent over the limited range of present interest. However, it is experimentally found that best differential capacitance curve fitting is obtained with $b \propto T^{-2}$, in agreement with the predictions of rows two and three and in approximate agreement with the single-image result. Further complexity would have to be added to the present theories to resolve this apparent discrepancy between the temperature dependences of $a$ and $b$. Since Pople[75] has found good agreement between the experimental temperature dependence of the dielectric constant of bulk water and that calculated from a theory which involves bendable hydrogen bonds and association, it is possible that changes of planar association with temperature may explain much of the present discrepancy. Finally, it is worth mentioning that the image-theory temperature dependence may vary appreciably with the distance $S$. For example, the value $S=3$ A leads to a value of 1.372 for $\nu$ in the infinite image case.

It is often stated or assumed that the first adsorbed layer of molecules having a permanent dipole moment is completely aligned in one direction with the dipole vector normal to the surface.[76] Such alignment corresponds to complete dielectric saturation, so that $\epsilon=\epsilon_\infty$. In our present terms, it requires that at the temperature of interest $\langle W_a \rangle \gg kT$, in disagreement with our results. If the molecules of the inner layer were completely aligned with no external field applied and if $\epsilon_\infty=6$, the largest likely value, the experimentally required value at the ecm of the inner-layer capacitance $C_1$ which is about 32 $\mu$f/cm$^2$ for water at 0°C (assuming no specific adsorption at this point), would lead to an inner-layer thickness of only 1.66 A, far too small a value. Further, the addition of an external field could produce no more dielectric saturation, and the decrease in $C_T$ and $C_1$ found on cathodic polarization could not be explained as arising from further saturation. For the same reasons, it is not possible to obtain even rough agreement with experiment on assuming that there is a sufficiently large "natural" field to cause $\epsilon_1$ at the ecm to have reached its required value[77] of about 15 solely because of dielectric saturation down from the 25°C bulk value of 78.3. Our present methods of justifying this low value are greatly preferable since they do not depend on such great initial saturation and take into account, directly, differences in behavior between the inner layer of solvent molecules and such molecules in bulk.[78]

At the ecm and for the concentration range considered in the present work, most water molecules in the inner layer will not have a solute ion next to them. For those that do, however, there will be some dielectric saturation from the ion field, especially in the region around positive ions.[47] Since positive ions produce more saturation than negative, this effect will not be symmetric in $E_1$, but will become more important for cathodic than for anodic polarization. Since increased ionic concentration next to the inner layer is associated with an increased field magnitude in the inner region, the foregoing field-dependent treatment of dielectric saturation will also account for this ionic saturation. The differing effects of positive and negative ions would require somewhat different values of $b$ for positive and negative polarization, however. Some of the asymmetry about the ecm which has been attributed to the anisotropic binding energy $W_a$ probably arises from this difference. However, since the ionic-saturation effect is concentration dependent and curve fitting without it yields good agreement in the region of the ecm, to the present order of approximation the ionic-saturation effect need not be considered separately from the other saturation effects in the inner layer.

## INNER-LAYER EQUATIONS OF STATE AND COMPRESSION

The electric field produces a pressure in the inner region which in turn affects such properties of the inner region as dielectric constant and thickness. We first consider, phenomenologically, the dependence of these properties upon pressure and then shall determine the dependence of pressure upon electric field. If one replaces linear terms in existing approximate

[75] J. A. Pople, Proc. Roy. Soc. (London) **A205**, 163 (1951).
[76] A. R. Miller, *Adsorption of Gases on Solids*, (Cambridge University Press, Cambridge, England, 1949), p. 105.
[77] Here we are in complete agreement with Mott and Watts-Tobin,[30] although the agreement is somewhat fortuitous considering the uncertainties in the values of $\epsilon_\infty$ and $d_0$. The present work assumes a larger value of $\epsilon_\infty$ than does the work cited.
[78] Again we are in complete accord with Mott and Watts-Tobin.[30]

phenomenological equations of state[79–83] by logarithmic ones, one obtains the following results[22i] which avoid earlier difficulties of negative quantities at high pressures:

$$V_0/V \equiv \lambda \equiv \rho/\rho_0 = (1+m\alpha p)^{1/m}, \tag{28}$$

$$\epsilon/\epsilon_0 = (1+m\alpha p)^{n/m} = (V_0/V)^n = \lambda^n, \tag{29}$$

where $\rho$ is the density, and the following simplifying relations have been introduced:

$$\left.\begin{aligned} p &\equiv P - P_0, \\ m &\equiv V_0/C \log e, \\ n &\equiv mA\epsilon_0 \log e = A\epsilon_0 V_0/C, \\ \alpha &\equiv [m(P_0+B)]^{-1}. \end{aligned}\right\} \tag{30}$$

The essentially temperature independent constants $A$ and $C$ and the pressure independent constant $B$ are parameters appearing in the approximate Tait,[80,81] and Owen-Brinkley[82–83] equations of state, and $P_0$ and $V_0$ are the initial reference pressure and volume. The quantity $\epsilon_0$ is the dielectric constant at the pressure $P_0$. Equation (28) yields the following result for the instantaneous compressibility,[22j]

$$-V^{-1}(\partial V/\partial P)_{T_0} \equiv \beta_T(P) = \alpha/[1+m\alpha p]. \tag{31}$$

When Eq. (28) is applied to Bridgman's data[84] for bulk water, excellent fits may be obtained.[85] There is no way to transform (28) so that both $m$ and $\alpha$ can be obtained simultaneously from least-squares fitting, but $\alpha$ may be so obtained for given $m$. When such a procedure is carried out, it is found that the value of $m$ which leads to the highest $r_t^2$ and lowest sum of squared deviations $S_s$ simultaneously yields a value of $\alpha$ in excellent agreement with independently measured values of $\beta_T(1)$. As an example, the best $m$ for the 0°C data is 6.58, $r_t^2$ is 0.999997, and $S_s$ is $6.42\times10^{-5}$. The value of $\alpha$ obtained is $5.06\times10^{-11}$ cm²/d, which may be compared with Marshall, Staveley, and Hart's[86] value of $5.04\times10^{-11}$ cm²/d. Since there are no points in Bridgman's data for pressures between 0 and 500 kg/cm², Eq. (28) performed a very long extrapolation almost perfectly in yielding $5.06\times10^{-11}$ cm²/d as the best value at 0°C.

For bulk water, curve fitting such as that discussed above shows that $m$ is not entirely temperature independent but decreases to about 6 by 15°C and remains nearly constant above this temperature.[85] The techniques of comparison with measured values of $\beta_T(1)$ and/or determination of $m$ to give least-squares data fitting are unavailable for the material in the inner layer, whose free volume is certainly different from that of bulk solvent. This fact will unquestionably make the inner-layer $\alpha$ smaller than that of bulk material, but its effect on $m$ is unknown. Therefore, we select $m=1$ as the temperature-independent value to be used in almost all of the curve fitting. Such a choice, while it does not yield quite as close a fit as will higher values, eliminates one disposable constant from the curve fitting and is consistent with the results of linear stress-strain analysis, as is shown later. Even for bulk water, the choice $m=1$ still leads to an $r_t^2$ of 0.991 for the 0°C Bridgman data.

Equation (29) involves $\epsilon$; actually pressure can affect only the polarization, which is proportional to $(\epsilon-1)$. Therefore, an improved version of (29) is

$$\epsilon - 1 = (\epsilon_0 - 1)\lambda^n. \tag{32}$$

Using Bridgman's data[84] for $\lambda$ as a function of $P$, and the dielectric constant-pressure data of Kryopoulos[87] and Scaife[88] for bulk water at 20°C, least-squares analysis using (32) yields $n=1.313$, $S_s=4\times10^{-5}$, and $r_t^2=0.9998$. Because of the high value of $\epsilon$ for water, a similar analysis using (29) yields virtually identical results. Jacobs and Lawson[89] have analyzed experimental data for a variety of polar liquids and find that $d(\ln\epsilon)/d(\ln\rho)$ is a positive number very nearly constant over a wide range of pressure. Equation (29) yields just $n$ for the value of the above derivative, while (32) leads to $n=d[\ln(\epsilon-1)]/d(\ln\rho)$. The value of $d(\ln\epsilon)/d(\ln\rho)$ for water at 20°C quoted by Jacobs and Lawson was $1.34\pm0.02$. They find that the derivative seems to be somewhat temperature dependent for some polar liquids. Note that since $a \gg \epsilon_\infty$ for water, the above results measure almost entirely the pressure dependence of the dipole contribution to $\epsilon$.

There are no data on the pressure dependence of $\epsilon_\infty$ itself for water since such results would require combined pressure and microwave measurements. A small number of data on the dependence of the refractive index at 25°C on pressure are available,[90] however, and can be fitted by (32) with $\epsilon$ replaced by the square of the refractive index. The result is $n=1.102$ and

[79] W. Wien and F. Harms, *Handbuch der Experimentalphysik*, (Akademische Verlagsgesellschaft, Leipzig, 1926), Vol. VIII, part 2, pp. 224–228.
[80] P. G. Tait, *Physics and Chemistry of the Voyage of H. M. S. Challenger*, (Her Majesty's Stationery Office, London, England, 1888), Vol. II, part IV. S. P., LXI.
[81] H. S. Harned and B. B. Owen, *The Physical Chemistry of Electrolytic Solutions* (Reinhold Publishing Corporation, New York, 1958), p. 163, 379–381.
[82] B. B. Owen and S. R. Brinkley, Jr., Phys. Rev. **64,** 32 (1943).
[83] E. Hückel and E. Ganssange, Z. Physik. Chem. **12,** 110 (1957).
[84] P. W. Bridgman, Proc. Am. Acad. Sci. **48,** 309 (1912).
[85] A more detailed discussion will be published separately.
[86] J. G. Marshall, L. A. K. Staveley, and K. R. Hart, Trans. Faraday Soc. **52,** 19 (1956).
[87] S. Kryopoulos, Z. Physik **40,** 507 (1926).
[88] B. K. P. Scaife, Proc. Phys. Soc. (London) **B68,** 790 (1955).
[89] I. S. Jacobs and A. W. Lawson, J. Chem. Phys. **20,** 1161 (1952).
[90] J. S. Rosen, J. Opt. Soc. Am. **37,** 932 (1947).

$r_i^2=0.9997$. Note that this value of $n$ applies to only the electronic contribution to the distortion polarization.

There is no *a priori* reason to expect that the pressure dependence of the distortion and dipole parts of the polarization will be the same, and the foregoing results show that there is, indeed, a difference between the electronic and dipolar parts for bulk water. The two effects can be separately accounted for by modifying Eq. (5′) along lines suggested by the form of (32). The resulting more general formula is

$$\epsilon-1=\lambda^n(\epsilon_\infty-1)+\lambda^r ah(E), \tag{33}$$

where $r$ is a new constant which may differ from $n$, and the present additive combination of the distortion and dipolar contributions is clearly an approximation.[22k] The $a$ in (33) is defined at the reference pressure $P_0$ and its density dependence included in the $\lambda^r$ term. All the pressure measurements cited have been made, of course, with $E=0$ and the differential dielectric constant (there equal to the static constant) measured. The distortion polarization is proportional to $(\epsilon_\infty-1)$ and in the inner layer should depend directly on density, not specifically on dipole concentration, suggesting that $n=1$ would be the best value to use in (33). The value $n=1$ is also in good agreement with the 1.102 found for the electronic contribution in bulk water. Therefore, we shall use a temperature-independent value of unity for $n$ throughout the differential capacitance calculations.

Let us now consider the inner layer as a continuous spherical shell surrounding a compressible mercury drop. Denote the average shell isothermal compressibility at zero applied field as $\beta_E$, where the subscript $E$ is used to suggest that the compressibility of a material in an electric field will not necessarily equal that obtained from direct pressure measurement. Then, by definition $\beta_E=-V^{-1}(\partial V/\partial P_E)_T$, where $P_E$ is the electrostatic pressure and $\beta_E$ is evaluated at $E_1=0$. Using linear elasticity theory for a continuous isotropic medium, we have carried out a detailed analysis of the compression of a spherical shell surrounding a compressible sphere for arbitrary sphere radius and shell thickness and for arbitrary radial pressures. The result is complicated and will not be given here. In the present case, the shell thickness is many orders of magnitude smaller than the sphere radius and great simplification can be made in the results. In particular, it turns out that, as expected, the compressibility of the mercury, even if it were much greater than that of the inner layer, would not enter into the final results for the layer compression.

If $P_E$ is the constant electrostatic pressure acting in the inner region, then the simplified results of the linear analysis may be expressed as

$$(V-V_0)/V_0=(t-t_0)/t_0=-(\beta_E/3)[(1+\sigma)/(1-\sigma)]P_E, \tag{34}$$

where $\sigma$ is Poisson's ratio for the inner region and $V=V_0$ at $P_E=0$. By definition, $t_0=1$. We have taken the initial volume to be that with hydrostatic pressure from the bulk of the solution acting but with no electrostatic pressure. Thus, one may identify $P_E$ and the $p$ of Eq. (28). Without any change to first order and hence without a change in the results of the linear analysis, one may now replace the $V_0$ and $t_0$ in the denominators of (34) by $V$ and $t$. Then we obtain

$$V_0/V=t_0/t=1+\alpha P_E, \tag{35}$$

where we have set

$$\alpha\equiv(\beta_E/3)[(1+\sigma)/(1-\sigma)], \tag{36}$$

a quantity which depends only weakly on temperature and which will here be taken independent thereof.[22l] Note that (35) is of exactly the form (28) with $m=1$. Thus, thel inear stress–strain analysis yields results entirely consonant with the linear version of the modified Tait equation (28) which we shall use.

The value of $\sigma$ appropriate for the inner region is unknown. However, the value for ice[91] is about 0.37, and the use of the reasonable value $\frac{1}{3}$ for $\sigma$ in (36) yields $\beta_E=1.5\alpha$. Although $\beta_E$ is the average electrically determined compressibility of the inner region, this region is really not entirely homogeneous. We have assumed that the thickness when $P_E=0$ is made up, for water solvent, of about 3 A from a water molecule and 1.4 A coming from parts of a surface mercury atom and of a closest-neighbor solute ion. If we assume that the material of the atom and ion is incompressible compared to the water molecule, then the compressibility of the latter in the inner layer $\beta_w$ is given by $\beta_w=4.4\beta_E/3$. Using $\sigma=\frac{1}{3}$, $\beta_w\cong 2.2\alpha$. For methanol using 5.4 and 1.4 A and $\sigma=\frac{1}{3}$, $\beta_m\cong 2\alpha$.

Later curve fitting yields $\alpha=1.7\times10^{-11}$ cm²/d for water solvent and $8.5\times10^{-11}$ cm²/d for methanol solvent. When these values are combined with the above results, one obtains $3.7\times10^{-11}$ and $17\times10^{-11}$ cm²/d for the approximate compressibility of water and methanol molecules, respectively. These values should be compared to $4.57\times10^{-11}$ and $12.6\times10^{-11}$ cm²/d, the bulk values for water and methanol, respectively, at 25°C. Because of the greatly reduced free volume in the inner layer as compared to that in bulk solvent, the values of the "single-molecule" compressibility $\beta_w$ and $\beta_m$ should be smaller than the values for bulk water and methanol. Even for water, where this is actually the case, it appears that $\beta_w$ is somewhat larger than might be expected, but in view of the uncertainties which went into the calculation of these quantities, the final values are not surprising. Note that when the free volume is reduced or eliminated, the application of pressure actually involves the

[91] Reference 41, p. 446.

compression of the molecules themselves, a process discussed by Bridgman[92] and Macleod.[93]

It will be noted that (34) or (35) shows that the relative change in inner-layer volume equals the relative thickness change. If we consider a physical dipole in such a situation, the change in volume when pressure is applied will increase the amount of matter per unit volume and will thus increase the dipole contribution to $\epsilon$. This effect is taken into account in the $\lambda^r$ term of Eq. (33). At the same time, the decrease of inner-layer thickness will decrease the effective charge separation of the dipole and will thus decrease $\mu_v$. The two effects will nearly cancel on the average. Thus, it appears that for the inner layer it is best to include no dependence of the dipolar dielectric constant contribution on volume and to take $r=0$. This choice yields a slightly better fit between theory and experiment than does taking $r=1$, and it also leads to somewhat larger values of $\alpha$ than are required by the latter choice. Note that the reduction in $\mu_v$ with decreasing thickness affects the rapidity with which dielectric saturation occurs but has not been included explicitly in our saturation calculations. It can be approximately accounted for by making a slight increase in the theoretical values of $b$ given in Table I, bringing them closer to the value required for good curve fitting.

## PRESSURE AND ELECTROSTRICTION

The electrostatic pressure in the inner region arises from two effects. One is the direct compressive effect of the diffuse layer. To the degree that this region can be considered to produce a capacitance in series with that of the inner layer, it can also be considered as producing an effective capacitor plate at the outer Helmholtz plane having equal and opposite charge to that of the electrode, the other plate of the inner-layer capacitance.[40] The two oppositely charged "plates" will attract each other and exert a pressure on the intervening material. Only this effect was considered in I.

"Electrostriction" is generally used to denote the change in pressure occurring in a dielectric fluid subjected to an electric field. Grahame[39] has, however, used electrostriction to mean the distortion of a solvent molecule with separation of its charge centroids and consequent increase in the effective dielectric constant. This process will almost always be overshadowed by the compressive effect of electrostriction as it is commonly understood. As discussed in the last section, it even appears that compression may, in some instances, lead to a reduction in dipole moment and little or no over-all change in dielectric constant. Grahame[3] has later adopted the more usual view that the principal result of electrostriction is a compression which, in the present case, will lead to a reduction in inner-layer thickness. The last section has shown that any pressure, electrostrictive or not, may lead as well to an increase in effective dielectric constant arising from increased density and an increased number of dipoles per unit volume. All of these effects are taken into account in the present treatment.

Let us again consider the experimental system with spherical symmetry. Such symmetry leads to an electric field which varies through the thickness of the inner layer. If $R_1$ is the radius of the mercury sphere and $R_2$ that to the outer surface of the inner layer,the outer Helmholtz "plane," then since $R_1$ and $R_2$ differ exceedingly slightly, it will be an excellent approximation to take the density and dielectric constant independent of position through the inner layer since the field will actually vary only infinitesimally. These assumptions should make our results agree exactly with those for a plane layer in the limit $R_2 \rightarrow R_1$. Let us further make the approximation introduced earlier that the dielectric constant abruptly changes from $\epsilon_1$ in the inner region to $\epsilon_2$ just beyond its outer boundary. The actual variation will be rapid but not a step function. Finally, assume a charge $q$ on the mercury and a charge $-q$ on the total diffuse layer replaced by an equivalent conducting shell at a distance $R_3$.

To calculate the pressure, we first find the Helmholtz free energy $\Phi$ given by $\Phi \equiv U - TS = U_{\text{elec}} - TS_{\text{elec}} + U_{\text{mech}} - TS_{\text{mech}}$. Here we have broken the energy and entropy into electrical and mechanical parts, a procedure valid to at least first order. Defining the three pressures $P_1$, $P_2$, $P_3$ at $r=R_1$, $R_2$, $R_3$, these quantities may be calculated from the relation

$$P_i = -(\partial\Phi/\partial V)_{T,R_j,R_k,E,N}, \tag{37}$$

where $i, j, k$ are any permutation of 1, 2, 3. Expanding $\Phi$ as before, the pressure consists of two terms $P_i = (P_H)_i + (P_E)_i$, where $(P_H)_i$ is the hydrostatic pressure, $(P_E)_i = -(\partial U_{\text{elec}}/\partial V)_{T,R_j,R_k,E,N}$, and it is assumed that $(\partial S_{\text{elec}}/\partial V)_{T,R_j,R_k,E,N} = 0$.

The electrostatic pressure may now be calculated from the electrostatic energy

$$\begin{aligned} U_{\text{elec}} &= (8\pi)^{-1}\int (D_1^2/\epsilon)\,dV = \tfrac{1}{2}\int_{R_1}^{\infty} (r^2 D_1^2 dr/\epsilon) \\ &= \tfrac{1}{2}q^2\int_{R_1}^{\infty} (dr/\epsilon r^2) \cong \tfrac{1}{2}q^2\left[\epsilon_1^{-1}\int_{R_1}^{R^2} (dr/r^2) + \int_{R_2}^{R_3} (dr/r^2)\right] \\ &= \tfrac{1}{2}q^2[\epsilon_1^{-1}(R_1^{-1} - R_2^{-1}) + \epsilon_2^{-1}(R_2^{-1} - R_3^{-1})], \end{aligned} \tag{38}$$

where $D_1$ is the displacement associated with $q$.

Taking proper account of signs and simplifying the final results by setting $R_1/R_2 \cong 1$, one finds

$$(P_E)_1 = (\epsilon_1 E_1^2/8\pi)\{1 + [\partial(\ln\epsilon_1)/\partial(\ln\lambda)]_{T,E,N}\}, \tag{39}$$

$$(P_E)_2 = (\epsilon_1 E_1^2/8\pi)\{1 + [\partial(\ln\epsilon_1)/\partial(\ln\lambda)]_{T,E,N} - (\epsilon_1/\epsilon_2)\}. \tag{40}$$

[92] P. W. Bridgman, Revs. Modern Phys. **7**, 1 (1935).
[93] D. B. Macleod, Trans. Faraday Soc. **40**, 439 (1944).

The direct contribution from the diffuse-layer ions is

$$(P_E)_3=(\epsilon_2E_2^2/8\pi)=(\epsilon_1^2/\epsilon_2)(E_1^2/8\pi). \quad (41)$$

If we consider $R_3$ to be slightly greater than $R_2$ and then let it approach the latter, the total pressure at $R_2$ will be $[(P_E)_2+(P_E)_3]$, equal to $(P_E)_1$, and the pressure is thus constant within the inner layer. Let us therefore identify $(P_E)_1$ and the $P_E$ previously introduced.

Equation (39) for $P_E$ admits a most simple interpretation. Its first term is just the force per unit area between two oppositely charged capacitor plates with a medium of dielectric constant $\epsilon$ between them. The second term is the usual expression for electrostriction[94–96] for the case of position-independent density ($\lambda\equiv\rho/\rho_0$). Petukhov has devised a direct method of measuring this term in liquids.[97]

When the general expression (33) is used for $\epsilon_1$ and substituted in (39), one obtains

$$P_E=(E_1^2/8\pi)[1+(1+n)\lambda^n(\epsilon_\infty-1)+(1+r)\lambda^r ah(E)], \quad (42)$$

which combines compression, electrostriction, and dielectric saturation. If $E_1$ is given in volts per centimeter, (42) may be rewritten as,

$$P_E=4.42708\times10^{-7}E_1^2[1+(1+n)\lambda^n(\epsilon_\infty-1)+(1+r)\lambda^r ah(E)] \quad (\mathrm{d/cm^2}). \quad (42')$$

We also have

$$\lambda=(1+m\alpha P_E)^{1/m} \quad (28')$$

from (28). Equations (42) and (28′) must be solved together by iteration in the general case of arbitrary $n$, $r$, and $m$. Such iteration has been included as part of the computer program for the present problem and is found to converge rapidly in the range of interest. The interlocking of (42) and (28′) is a kind of positive feedback, since an increase in pressure increases $\lambda$ which in turn, increases pressure further. In the present case, we shall usually take $m=n=1$, $r=0$, and we may then solve directly for the pressure to give

$$P_E=\frac{(E_1^2/8\pi)[2\epsilon_\infty-1+ah(E)]}{1-2\alpha(\epsilon_\infty-1)(E_1^2/8\pi)}. \quad (43)$$

The feedback factor in the denominator must not vanish, and this condition sets an upper limit on the permissible $E_1$ for which the equation is at all pertinent. This upper limit is not approached in the present curve fitting. In an actual liquid, $m$ will considerably exceed unity and the feedback will be far less strong for high $E_1$.

It is important to note that in the derivation of (39) to (41) chemical potential is not held constant after the electric field is switched on. It will also be noted that (39) involves $E_1$ rather than $E=E_0+E_1$. $P_E$ is, therefore, the equivalent pressure arising from the applied field only. The difference in dipole image attraction with positive and with negative poles next to the electrode is expressed by the effective field $E_0$. This difference itself will lead to an average adsorption pressure which is certainly not homogeneous but may still be evaluated approximately from (39) with $E_0$ replacing $E_1$. Using the value of $E_0$ determined from curve fitting for water solvent, the resulting pressure $P_E^\circ$ is about 20 atm. It is probably more accurate to refer the initial layer volume and compressibility to this pressure rather than to 1 atm, but the actual differences caused thereby are completely negligible for present purposes.[22m]

## FINAL FORMULAS

Equation (4) for $C_1$ involves the quantity $dq/dE_1$ and functions of the normalized layer thickness $t$. The results necessary to calculate $C_1$ will be given in this section in complete generality even though for curve fitting we shall usually use $m=n=1$ and $r=0$.

In earlier sections we have taken $q=\epsilon_1E_1/4\pi$, thus eliminating any contribution from $D_0$ to $q$. It immediately follows that

$$dq/dE_1=(4\pi)^{-1}[\epsilon_1+E_1(d\epsilon_1/dE_1)]$$
$$=(4\pi)^{-1}[(E_1/E)\kappa_1+(E_0/E)\epsilon_1]. \quad (44)$$

Thus, $C_1$ involves both $\kappa_1$ and $\epsilon_1$. When $\kappa_1$ is obtained from the expression for $\epsilon_1$, the result is complicated because of the dependence of $\epsilon_1$ on $E_1$ through $\lambda$ and $P_E$ and on $E$ through $h(E)$. The following quantities will therefore be introduced to simplify the formula for $\kappa_1$:

$$\left.\begin{aligned} A_1&\equiv\lambda^n(\epsilon_\infty-1),\\ B_1&\equiv\lambda^r ah(E),\\ F_1&\equiv\lambda^r ag(E),\\ G_1&\equiv\frac{\alpha P_E(nA_1+rB_1)[2(E/E_1)(1+n'A_1+r'B_1)+r'(F_1-B_1)]}{\{1+m\alpha P_E+n'A_1[1+(m-n)\alpha P_E]+r'B_1[1+(m-r)\alpha P_E]\}}, \end{aligned}\right\} \quad (45)$$

[94] E. V. Condon and H. Odishaw, *Handbook of Physics* (McGraw-Hill Book Company, Inc., New York, 1958), p. 4–8.
[95] W. F. Brown, Jr., Am. J. Phys. **19**, 290 (1951).
[96] B. K. P. Scaife, Proc. Phys. Soc. (London) **B69**, 153 (1956).
[97] V. A. Petukhov, Soviet Phys.—Acoustics **4**, 294 (1958).

where $n' \equiv 1+n$ and $r' \equiv 1+r$. In the curve fitting the expressions for $g(E)$ and $h(E)$ given in Eqs. (18) and (19) will be used, but the results below are independent of the specific forms of these functions.

A number of the previously derived equations, as well as those for $\kappa_1$ and $d(\ln t)/d(\ln|E_1|)$, can be expressed in terms of the above quantities. The pertinent results, which include saturation, electrostriction, and compression effects, are summarized below:

$$P_E=(E_1^2/8\pi)[1+n'A_1+r'B_1],$$
$$\epsilon_1=1+A_1+B_1,$$
$$\kappa_1=1+A_1+F_1+G_1,$$
$$[d(\ln t)/d(\ln|E_1|)]=-|E_1/E|(G_1/[nA_1+rB_1]). \tag{46}$$

The following calculation procedure may now be employed. First, a value of $E_1$ is selected and $V_1$ calculated. Then $P_E$, $\epsilon_1$, and $\lambda$ are obtained by iteration. The quantities $q$ and $E_2$ may then be calculated, and Eqs. (1) and (2) used to give $C_2$ and $V_2$. The potential $V_0$ follows from $V_1$ and $V_2$. Finally, Eqs. (4) and (44) are combined to yield $C_1$, and the total differential capacitance $C_T$ is calculated. The static or integral capacitances may also be readily obtained and are, in fact, part of the standard digital computer output.

If there were no electrostriction, the term $G_1$ in $\kappa_1$ would be zero. This added term is relatively small under all conditions and only reaches a value slightly greater than unity at the extremes of the experimental range of differential capacitance measurements. Note that $G_1/(nA_1+rB_1)$ is not zero, however, in the absence of electrostriction provided the inner layer is compressible. The term $|E/E_1|$ which appears in the expression for $G_1$ and that for $d(\ln t)/d(\ln|E_1|)$ arises because $E$ not $E_1$ appears in the relation between $g(E)$ and $h(E)$ and because $P_E$ involves $E_1$ rather than $E$. This ratio will be very close to unity for large $E_1$ and the values of $E_0$ used herein, and the terms in which it appears will be completely negligible for small $E_1$. In addition, $G_1$ and $d(\ln t)/d(\ln|E_1|)$ are small correction terms to begin with. Thus, the presence or absence of $|E/E_1|$ has very little influence on the formulas or curve fitting. If $P_E$ were taken proportional to $E^2$ rather than $E_1^2$, the terms involving $|E/E_1|$ would disappear from the formulas and best curve fitting would be achieved with a value of $\alpha$ less than 5% smaller than presently required. In addition, over most of the range where dielectric saturation is appreciable, $E_1/E$ in (44) will be nearly unity and $E_0/E$ nearly zero. Because of the uncertainty in the field dependence of the dielectric saturation functions, the small difference between $\kappa_1/4\pi$ and the expression (44) has been ignored in some of the curve fitting. Its inclusion leads to slightly larger values of $b$ than those given.

Dielectric saturation leads to a final decrease in $h(E)$ proportional to $E^{-1}$. Sensible values of $r$ and $m$ will always be such that the electrostrictive contribution to $B_1$ and $F_1$ will not outweigh this decrease. Thus, it may be assumed that these quantities will go to zero as $E_1$ and $P_E$ increase without limit. The correction term $G_1$ is still not limited as $E_1$ increases, however, but will continue to increase because of the factor $\lambda^n$ which does not cancel out. If $m$ is greater than $n$, the usual case for liquids, the derivative $d(\ln t)/d(\ln|E_1|)$ will approach the constant $-2/(m-n)$ in the above limit. On the other hand, in the exceptional case $m=n$ the derivative goes to $2n'A_1/m$, an expression which increases indefinitely as $E_1$ increases. Since the derivative appears in Eq. (4) as $[1+d(\ln t)/d(\ln|E_1|)]^{-1}$, it is clear that it must be limited in magnitude to less than unity. The above results therefore suggest that unrestricted application of the present expressions requires $m>n$ and $[2/(m-n)]<1$. These conditions will be well met for all real liquids. For the present close-packed monolayer, we have generally used $m=n=1$ for simplicity and convenience. No trouble arises from this choice in the curve fitting since the maximum value of $|d(\ln t)/d(\ln|E_1|)|$ which occurs is less than 0.25.

## CURVE FITTING AND DISCUSSION

In this section we shall discuss the results of applying the foregoing theory to Grahame's experimental differential capacitance measurements on NaF in water[2,3] and KF in methanol[39] solvents. The data presented in the following curves have been plotted directly from Grahame's original smoothed strip sheets and should, therefore, preserve the high accuracy of the original measurements.[98] We have elected to compare theory and experiment using differential rather than static or integral capacitance curves. Integral curves are much smoothed and averaged by the integration process and thus fail to show the detailed fine structure which appears in the directly measured differential capacitance curves. Fitting of theory to integral curves is therefore a less precise and stringent test than is fitting to differential curves. We have also elected to compare with total double-layer capacitance rather than with Grahame's curves for $C_1$. The reason for this choice is the uncertainty in Grahame's procedure for calculating $C_1$. It will be shown that the series capacitance assumption is not generally correct; as a consequence, it is necessary to employ a detailed theory of the specific adsorption process in order to extract the inner-layer capacitance from the total capacitance data in the region of specific adsorption. Correspondingly, comparison of $C_T$ data with a theory omitting specific adsorption may bring to light discrepancies arising from several combined adsorption effects in addition to the direct effect upon inner-layer capacitance.

It will be noted that for both the water and methanol

[98] We are grateful to Dr. Roger Parsons of the University of Bristol for furnishing us with these data.

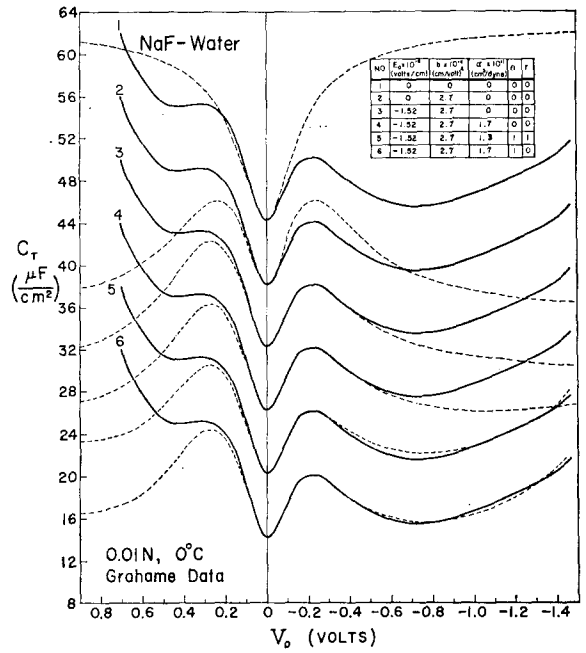


FIG. 2. Fitting of 0.01$N$, 0°C differential capacitance data for various assumptions. Curves displaced successively from bottom by 6 $\mu$f/cm$^2$.

solvents, the anion is $F^-$. As pointed out by Grahame and Soderberg[99] and by Grahame,[3] the fluoride ion, perhaps because of its size and low polarizability, seems to be the only univalent anion which exhibits little or no specific adsorption on mercury even with positive polarization. Thus it is the ideal, and, presently, the only choice available for comparison of experiment over a wide range of polarization with a theory, such as the present one, which includes no quantitative account of specific adsorption.

Grahame[100] has criticized the theory of I because it only yields differential capacitance curves symmetrical about the ecm, and so cannot give good agreement with experiment very far into the positive polarization region. This restriction is partly removed in the present work by the inclusion of the anisotropic binding energy of inner-layer molecules, but the results of this section show that still further assumptions will have to be made to attain agreement between theory and experiment very far into the positive region.

The detailed fitting of theoretical curves to Grahame's data has been carried out in the following way. For water it was decided to do the primary fitting using the 0°C data because the dielectric saturation and dipole constants $b$ and $a$ may be expected to increase with decreasing temperature. Thus, the variation in dielectric saturation with applied pressure differential should show up most strongly at the lowest available temperature, allowing its effect to be most accurately assessed there. Grahame's derived $C_1$ vs $q$ curve for 0°C does, in fact, show more structure, especially in the positive charge region, than do the results at higher temperatures.

Calculation of a theoretical curve using the digital computer required that the following constants be specified. For each solvent the temperature, normality, bulk dielectric constant $\epsilon_2$, saturated dielectric constant $\epsilon_\infty$, and ecm value of $d$, $d_0$, were taken as known, non-disposable constants. In addition, the values $n=m=1$ and $r=0$ were usually used. Then, the disposable constants $a$, $b$, $E_0$, and $\alpha$ had to be determined by trial and error and successive approximations. There was only slight interaction between the effects of changing the first three constants and that of changing $\alpha$; thus, the latter could be found quite rapidly once best values of the first three were determined.

The fitting was begun with the 0°C, 0.01$N$, water-solvent data. $E_0$ was selected to make the peak of the theoretical $C_1$ curve, the point of minimum dielectric saturation, occur at the charge value of the corresponding peak of Grahame's $C_1$ curve for this temperature. At 0°C, these peaks are well defined and a value of $x_0 \equiv \mu_v E_0/kT$ could be determined which is felt to be quite accurate. Variations in its value by 10% or more decreased the agreement between theory and experiment quite noticeably. With $\alpha=0$, a value of $a$ was then found which produced good agreement between the theoretical value of $C_1$ at the peak and Grahame's value. Then, values of $b$ were tried until good agreement with the experimental $C_T$ curve was attained in the region near the ecm where the effect of $\alpha$ was negligible. Finally, $\alpha$ was adjusted for best fit in

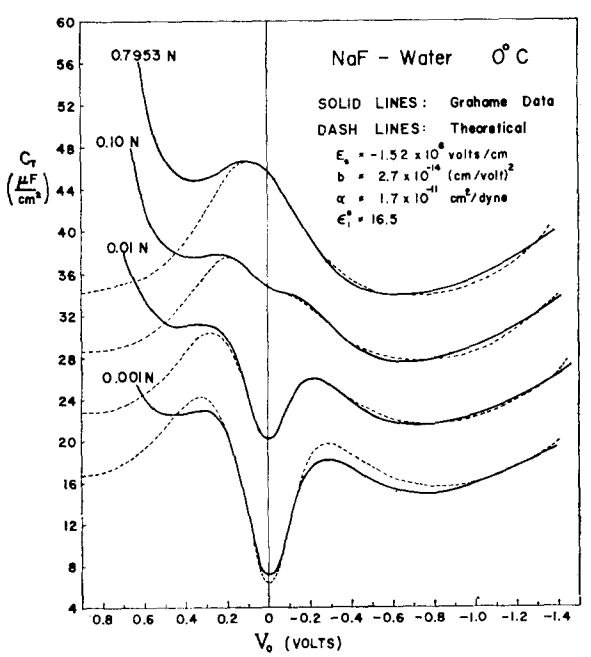


FIG. 3. Comparison of theory and experiment for NaF–water at 0°C.

[99] D. C. Grahame and B. A. Soderberg, J. Chem. Phys. **22**, 449, (1954).
[100] D. C. Grahame, Ann. Rev. Phys. Chem. **6**, (1955).

the region of high cathodic polarization. Although Grahame's $C_1$ curve was helpful in determining approximate values of the constants, their final values were established by successive trial and comparison against the experimental $C_T$ curve. It was found that when good agreement between theory and experiment was achieved for one concentration, very nearly the same degree of agreement could be expected on using the same constants to calculate a curve for a different concentration at the same temperature. This result again confirms the usefulness of the simple Gouy-Chapman diffuse-layer theory in the present situation up to high concentrations and justifies the assumed independence of inner-layer properties of solute concentration.

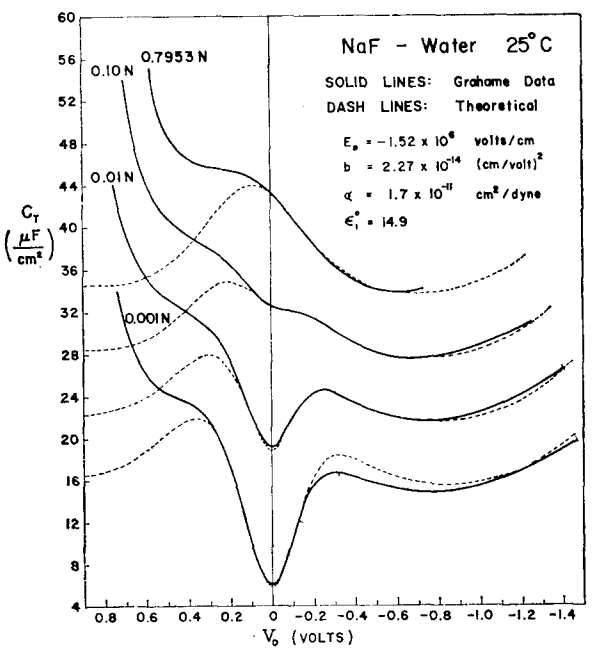


FIG. 4. Comparison of theory and experiment for NaF–water at 25°C.

Figure 2 illustrates the progressive improvement in the agreement between theory and experiment which can be achieved as various effects are included in the theoretical treatment. In this graph, the solid lines have been drawn from Grahame's data, and the dashed lines show how the theoretical results deviate. The solid vertical line near the center shows the position of the ecm. For convenience in illustrating various cases, the original data, represented by the bottom solid curve, have been repeated several times at 6 $\mu$f/cm² intervals. This separation of experimental curves for clarity will also be used in Figs. 3 to 7 and in Fig. 11.

In Fig. 2, curve 1 has been fitted by the combination of diffuse-layer theory and a constant inner-layer capacitance whose magnitude was selected to give agreement at the ecm. The great deviations over most of the range show the crudeness of the assumption of

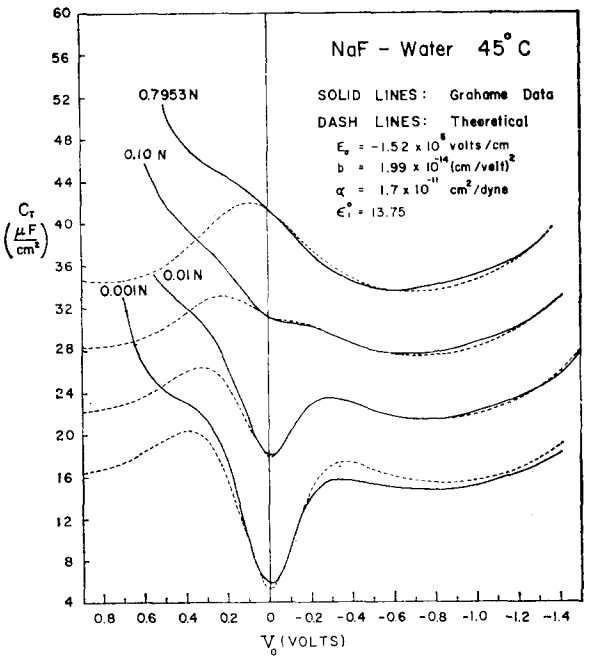


FIG. 5. Comparison of theory and experiment for NaF–water at 45°C.

constant $C_1$. As indicated in the data box on Fig. 2, curve 2 was calculated like curve 1 but with the addition of the final or best amount of dielectric saturation only. Note the symmetry of the dashed curve around the ecm. This symmetry disappears in curve 3 where the final value of $E_0$ has also been used in the calculation. In curve 4, the final value of the compression constant $\alpha$ has been included, but no electrostriction occurs since $n=r=0$. Layer compression

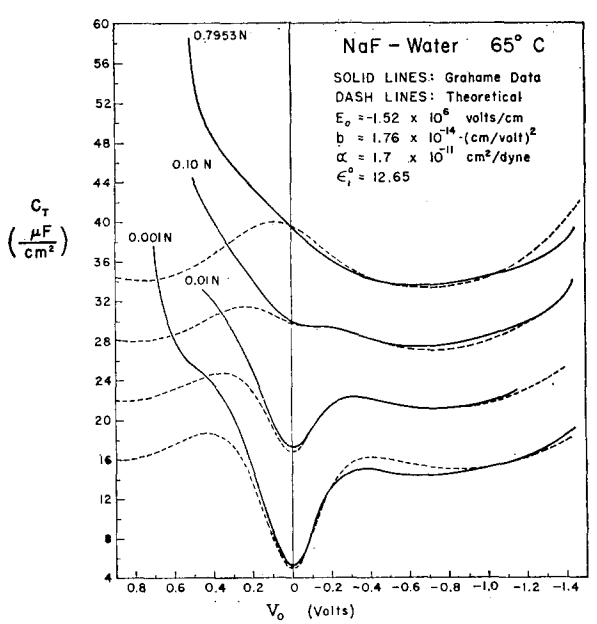


FIG. 6. Comparison of theory and experiment for NaF–water at 65°C.

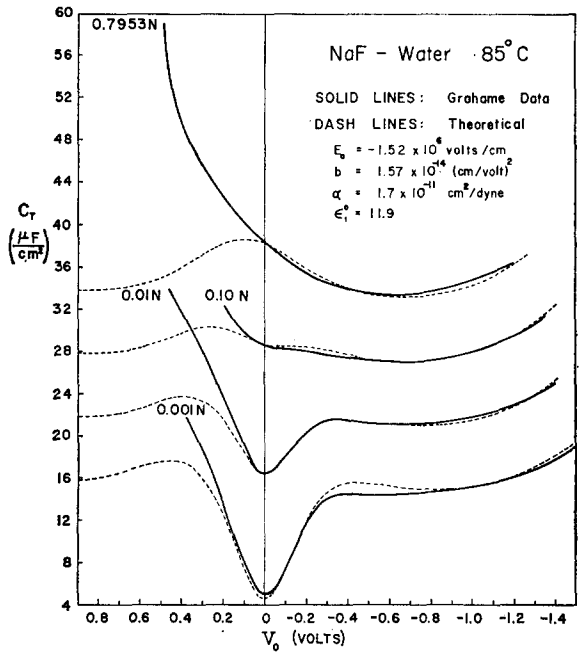


FIG. 7. Comparison of theory and experiment for NaF–water at 85°C.

alone has improved the agreement between theory and experiment considerably in the region of strong cathodic polarization, but a much larger value of $\alpha$ would be required, as was the case in I, to achieve close agreement in this region.

In curve 5, the values $n=r=1$ have been used together with the value of $\alpha$ which gives the best fit for this choice of $r$. Here, electrostriction is acting on both the distortion and dipolar contributions to the inner-region dielectric constant, and the best value of $\alpha$ is necessarily smaller than that required in the bottom curve where no dipolar electrostriction occurs and $r=0$. The values $m=n=1$, $r=0$ will be used hereafter. Curves 5 and 6 show that excellent agreement between theory and experiment can be achieved but that the agreement seems to be somewhat better when $r=0$.

Figures 3 through 7 show the curve fitting results for the principal temperatures Grahame used. They all indicate appreciable discrepancy between theory and experiment for the $0.001N$ curves in the intermediate range of cathodic polarization. Grahame's curve fitting showed similar deviations at this concentration, and he has ascribed them to experimental error,[2,39] which is more likely for dilute solutions than for concentrated solutions. There also seems to be a slight tendency for the high-concentration theoretical curves to drop off less rapidly for small cathodic polarization than do the experimental curves. This result suggests that the form of the function $g(E)$ given in Eq. (19) and used in the fitting does not allow fast enough dielectric saturation in this region. One explanation is that the single-image saturation results are most pertinent at low $V_0$'s, while the build up of more and more ions of a single sign next to the inner region tends to make the infinite image predictions begin to be more applicable at higher potentials. The transition from one towards the other would produce faster dielectric saturation than (19) can accommodate.

The main discrepancy in Figs. 3 to 7 is the failure of the theory to predict the experimental results over much of the positive polarization region. It is clear that some process not accounted for in the present theory produces a considerable increase in over-all capacitance as the electrode is made more and more positive. One possibility is that the inner layer is far more compressible for positive than for negative polarization, a physically unlikely assumption. Another is that rise in capacitance comes from pseudocapacitance[101] associated with the discharge of negative ions such as $OH^-$. This explanation must be discarded both because of the scarcity of $OH^-$ ions in the solution and because the characteristic frequency dependence associated with pseudocapacity was not found by Grahame and little discharge current was noted.

The most likely explanation seems to us to be that the extra capacitance comes from the specific adsorption of anions, possibly $F^-$ ions. Hackerman and Popat,[102] working with a platinum electrode, have mentioned that the anodic process occurring at the extreme left is oxygen, not fluoride, evolution. They suggest that fluorine ions are not dehydrated and that the main adsorption process in this case is that of $OH^-$ ions. A similar suggestion has been made by Wanklyn.[103] In addition to adsorbed hydroxyl ions, Watts-Tobin and Mott[30,53] also have suggested the possibility of adatom formation at the mercury surface as a means of explaining the anodic rise.

It is found that the character of the cations makes very little difference in differential capacitance measurements.[104] On the other hand, the type of anion makes a profound difference, especially when the electrode is positively charged.[105,106] There is general agreement that all electrolyte anions but $F^-$ are specifically adsorbed on mercury, and it seems somewhat unlikely to us that there is a major difference in kind on going to $F^-$. The differences in Figs. 3 to 7 between theoretical and experimental lines for high concentrations on positive polarization suggest that the added effect occurs for smaller electrode charges as the temperature increases. If the discrepancies shown arise from specific adsorption of anions in NaF, one may conclude that such adsorption is relatively independent of concentra-

[101] D. C. Grahame, J. Electrochem. Soc. **99**, 370C (1952).
[102] N. Hackerman and P. V. Popat, "Capacity of the Electrical Double Layer and Adsorption at Polarized Platinum Electrodes," Tech. Rept. to the Office of Naval Research (1958).
[103] R. J. Watts-Tobin (private communication).
[104] D. C. Grahame, J. Electrochem. Soc. **98**, 343 (1951).
[105] D. C. Grahame, M. A. Poth, and J. I. Cummings, J. Am. Chem. Soc. **74**, 4422 (1952).
[106] D. C. Grahame, Z. Electrochem. **59**, 773 (1955).

tion; it occurs more readily at higher temperatures; and it generally requires for its occurrence a higher positive electrode charge than necessary for other electrolytes.

The above temperature dependence follows, in the present picture, in part from the decreased binding of water molecules to the mercury at increased temperatures. They are thus easier displaced by anions at higher temperature, and the strong specific chemisorption of the anions replaces the largely physical adsorption of water molecules. On identifying the added capacitance as arising from specific adsorption, its approximate independence of electrolyte concentration is more difficult to explain and has been one of the reasons previously adduced against specific adsorption of $F^-$. On the other hand, such independence is a natural consequence of hydroxyl-ion adsorption, but the scarcity of $OH^-$ ions in the neighborhood of the mercury drop during its growth makes such adsorption seem unlikely at first. However, if the $OH^-$ ions come from inner-layer water molecules which lose hydrogens, a sufficient supply is directly available and $OH^-$ ion adsorption becomes a possible mechanism. Parsons[107] reports that the anodic rise is essentially unchanged on varying the $p$H from $p$H 7 to 11; but there is a large increase above $p$H 11. This would indicate that the specific adsorption of $OH^-$ ions, if it occurs, is also independent of the bulk concentration of these ions.

At the ecm, the present work requires that there be space-charge neutrality. As soon as the electrode acquires a charge, space charge will build up in the diffuse layer, and the layer of ions nearest the water molecules of the inner layer will be made up more and more of a single-charge type. The magnitude of the total unbalanced charge, or space charge, in the diffuse layer is approximately an exponential function of potential but only depends on the square root of electrolyte concentration. If we make the likely assumption that specific adsorption of $F^-$ is mediated most strongly by the concentration of anions in the space-charge layer next to the inner region, then for any appreciable positive potential it is easy to see why the magnitude of any specific adsorption of this ion, as measured by added capacitance, should depend strongly on potential but only weakly on bulk concentration. In fact, several plausible statistical models[21] lead to inner-layer properties which even in the presence of specific adsorption are potential sensitive and concentration insensitive.

Some clue concerning the dependence of the specific adsorption capacitance contribution on charge or potential may be obtained by considering the deviations of theory and experiment which occur in the positive polarization regions of Figs. 3 to 7. This problem will only be considered qualitatively at present. When an ion is adsorbed, it replaces a water molecule, and thus changes the average inner-layer capacitance, first because of the missing water molecule, and second because of its own contribution. In addition, the capacitance of the diffuse layer is changed slightly, but more important, the correct law for combining these two capacitances to arrive at $C_T$ is changed. If a fraction $(1-f)$ of the charges in solution is in the inner layer, the proper equation for the static capacitance is

$$C_T{}^s=[(V_1/q)+(V_2/q)]^{-1}=[(V_1/q)+f(V_2/fq)]^{-1}$$
$$=[(C_1{}^s)^{-1}+f(C_2{}^s)^{-1}]^{-1}. \quad (47)$$

In a similar manner one obtains for the differential capacitance,

$$C_T=\left[\frac{dV_1}{dq}+\frac{dV_2}{dq}\right]^{-1}=\left\{\frac{dV_1}{dq}+f\left[\frac{d(fq)}{dV_2}-q\frac{df}{dV_2}\right]^{-1}\right\}^{-1}$$
$$=\{C_1^{-1}+f[C_2-q(df/dV_2)]^{-1}\}^{-1}. \quad (48)$$

We see that even neglecting any effect of specific adsorption upon $C_2$, $C_T$ increases with specific adsorption by two mechanisms: the increase in $C_1$ from the adsorbed charge and the departure from the series-additivity law. Since $qdf/dV_2$ is probably negative, the latter effect is accentuated. Because of the implicit dependence of $f$ on $q$ and the total applied pressure differential, the actual application of the above equations requires a detailed theory of the specific adsorption process.[21]

If the final anodic rise in differential capacitance is attributed to specific adsorption of anions, the hump which appears at small anodic potentials at the lower temperatures may be ascribed to the conflicting effects of adsorption and dielectric saturation. As the anodic potential is decreased towards the ecm, electrode charge and specific adsorption decrease, causing the over-all differential capacitance to fall. At the same time, the inner layer becomes less dielectrically saturated, tending to make the over-all capacitance rise. The proportioning of these two effects can lead to the hump, and its disappearance at high temperatures can be explained by increased adsorption and decreased dielectric constant and saturation parameters $a$ and $b$. It is possible that the above explanation also applies to other, even larger humps found[3] with other solutes such as $KNO_3$.

It will be noted that the same values of $E_0$ and $\alpha$ have been used for all temperatures in Figs. 3 to 7. The values of $b$ used for temperatures above 0°C were obtained from that found at 0°C by applying the $T^{-2}$ dependence which follows from the usual dielectric constant theories, as shown in rows two and three of Table I. The only constant which was considered disposable in fitting the higher-temperature results was $a$. Little agreement with experiment could be achieved if $a$ was taken proportional to $T^{-1}$ or $T^{-1.3}$ (see Table I); so the value of $a$ for each temperature was chosen which yielded agreement at the peak of the cathodic hump

[107] R. Parsons, Proc. Roy. Soc. (London) **A261**, 79 (1961).

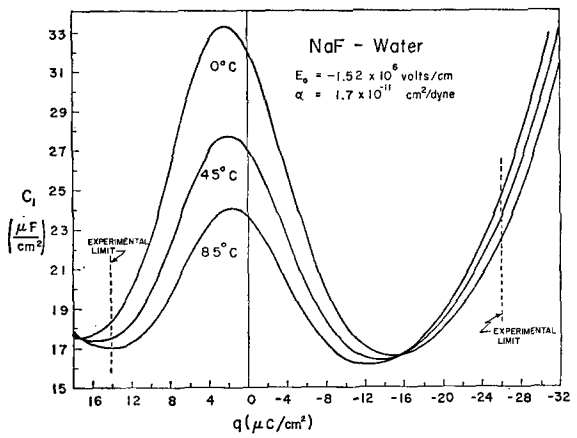


FIG. 8. Theoretically derived inner-layer differential capacitance vs electrode charge for three temperatures.

for the $0.01N$ curve. The resulting values of $a$ are quite consistent and indicate a temperature dependence with an exponent of approximately $-2$, as discussed earlier. No other $a$ and $b$ temperature dependence could be found which would yield good agreement with experiment over the entire range of temperature here covered. The consistency of agreement between theory and experiment is surprisingly good at all higher temperatures for fitting with only one disposable constant determined at only one point.

In most curves of Figs. 3 to 7, there seems to be a slight tendency for the theoretical results to lie above the experimental for extreme cathodic polarization. The deviation is usually hardly greater than experimental error and would have been even smaller had dielectric saturation in the diffuse layer been taken into account, but it may indicate that a somewhat larger value of $m$ than unity would be a better choice.

Once good agreement between theory and experiment is achieved, the dependence on potential, charge, or field of the various internal parameters of the system may be plotted. Figure 8 shows the dependence of the inner-layer differential capacitance on electrode charge for three temperatures. These results, in conjunction with diffuse-layer theory, lead to the agreement with experiment shown in the earlier figures. This agreement is poor for appreciable anodic polarization; therefore, in this region the theoretical charge $q$ in Fig. 8 differs from the experimental electrode charge obtained from the experimental differential capacitance by integration. Over the rest of the range, from about $q=+2$ to $-25$ $\mu C/cm^2$ where the agreement is good, the theoretical and experimental charge values virtually coincide. In this range, the curves of Fig. 8 agree well with the corresponding Grahame curves.[3] It is believed the present results, obtained from computer curve-fitting, may be slightly more accurate than Grahame's in the cathodic polarization region.

Figure 9 shows how another derived quantity, the potential of the outer Helmholtz plane, varies with applied potential. The former potential is approximately the same as the zeta potential of the electrokinetic theory.[106] It will be noted that $V_2$ begins to saturate before very high over-all potentials are applied. As $V_0$ increases, $C_2$ increases rapidly and limits the potential $V_2$ across the diffuse layer. The deviation between theory and experiment for anodic polarization will cause the anodic $V_2$ values shown in Fig. 9 to be somewhat uncertain, but the degree of error or uncertainty here is far smaller than that arising from the same cause in Fig. 8 because the diffuse layer capacitance and $V_2$ are much less sensitive to such deviations than is $C_1$. The present theoretical $0.1N$ curve is in good agreement with Grahame's[106] corresponding curve for KF.

Figure 10 illustrates the dependence on electrode charge and on the field $E_1$ of various inner-layer parameters derived from the 0°C curve fitting. Rather than plot the pressure directly, the part of it which depends on dielectric constant and electrostriction has been shown. The dotted lines indicate the behavior when $\alpha=0$, for which there is no layer compression or electrostriction. In this case, the normalized pressure curve becomes identical with the $\epsilon_1$ curve. The scale for the compression parameter $\lambda$ has been increased by a factor of 10, as indicated, in order to magnify its field dependence.

At the maximum internal field of about $3\times10^7$ v/cm, the layer has been compressed by about 10% and the electrostatic pressure has reached about 6000 atm. In I, a maximum compression of about 20% and pressure of 3000 atm were found. The reason for the difference is that the inclusion of electrostriction in the present work allows curve fitting with a much smaller value of $\alpha$ since less of the final rise in capacitance need come from direct layer compression.[22n] The effect of electrostriction shows up most strongly in Fig. 10 for the $\kappa_1$ curve, but it also has an appreciable effect on the $\epsilon_1$ and pressure curves at high fields. In particular, the final rise in the normalized pressure curve, which is just apparent at the highest fields, comes from the electro-

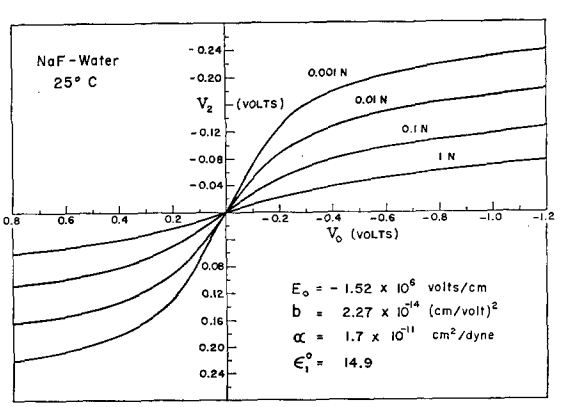


FIG. 9. Potential of the outer Helmholtz plane vs applied potential $V_0$ for four concentrations.

strictive increase in $\epsilon_1$. At high fields this increase begins to outweigh the saturation decrease because of the positive feedback factor discussed after Eq. (28′). Even at the highest fields this factor is small, however, and the necessary iteration converges to a final value in four or five cycles on the computer.

Accurate curve-fitting of the methanol-solvent results was more difficult than that for water solvent because data were available for only 25°C and because no anodic hump occurred. The absence of this hump makes the determination of $E_0$ very uncertain, and the resulting uncertainty has a direct effect on $a$ as well. Figure 11 shows the results of fitting the present theory to the methanol curves using $\epsilon_\infty = 4.5$ and $d_0 = 5.4$ A. It was found that a good fit near the ecm could be obtained with the same $E_0$ value used for water, and this is the value employed for the results of Fig. 11. As close a fit could also be achieved with either a considerably larger or somewhat smaller $E_0$, however, and the present value of $a$, 7.5, must also be considered quite approximate.

Because of the smaller $N_h$ and $\mu_v$ for a methanol rather than water monolayer, theoretical calculation of $a$ and $b$, such as that summarized in Table I for water, yields smaller values in the methanol case. Curve fitting leads to a considerably larger $b$ value for methanol than for water, however, in qualitative agreement with Malsch's experimental results for methanol and water.[70] Note that the value of $b$ found for the methanol monolayer, $11\times10^{-14}(\text{cm/v})^2$, is still smaller than Malsch's rather uncertain result for bulk methanol.

Again it is very probable that the final anodic rise in the differential capacitance comes from anion adsorption, as in the aqueous case. Grahame[39] presents capacitance curves in methanol solvent with $Cl^-$, $NO_3^-$, and $F^-$ as anions. The anodic-rise parts of the capacitance curves are extremely similar in these cases, with the main difference being that the rise occurs at higher anodic potentials as the solute is changed from $NH_4Cl$ to $NH_4NO_3$ to $NH_4F$. If the rise in KF from anion specific adsorption began in the low cathodic polarization region rather than in the anodic region or at the ecm, which is certainly a possibility, the fitting of much of the cathodic drop in capacitance by dielectric saturation, as in Fig. 11, would be incorrect, and the negative sign of $E_0$ here used might be wrong as well. In this case, a much smaller value of $b$ in better agreement with theoretical predictions, could be employed. In general, if specific adsorption effects can be separated from saturation effects, as was the case for water solvent at 0°C, much more accurate determination of $E_0$, $a$, and $b$ is possible than if such separation cannot be carried out. Because of the low freezing point of methanol, differential capacitance measurements using it as solvent should be possible at much lower than 0°C and, because of the increase in $a$ and $b$ and decrease in specific adsorption as temperature is reduced, a hump should appear at sufficiently low temperature, and this should allow the above separation to be carried out far better than is possible with the 25°C data.

The ratio between the initial isothermal compressibilities of bulk methanol and bulk water is 2.75 at 25°C, while that between the $\alpha$'s found here for the inner layer is about five. One possible reason for this discrepancy is that a considerable part of the bulk values arises from free-volume compression; thus, the ratio of individual molecular compressibilities can be,

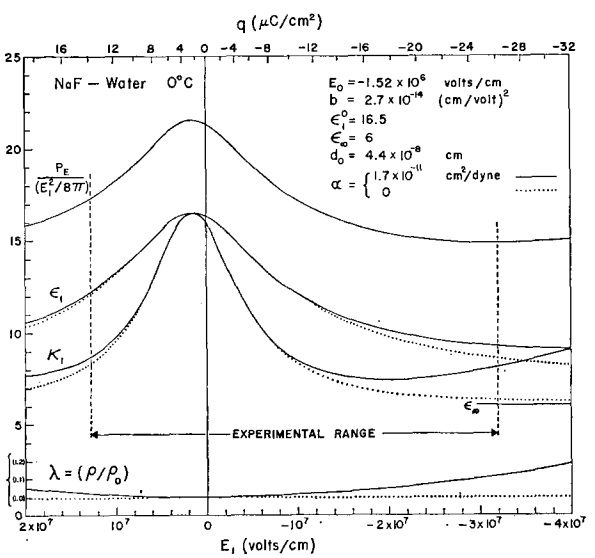


FIG. 10. Dependence of inner-layer parameters on electrode charge (top scale) and inner-layer field (bottom scale). Dotted lines show results without layer compression and electrostriction.

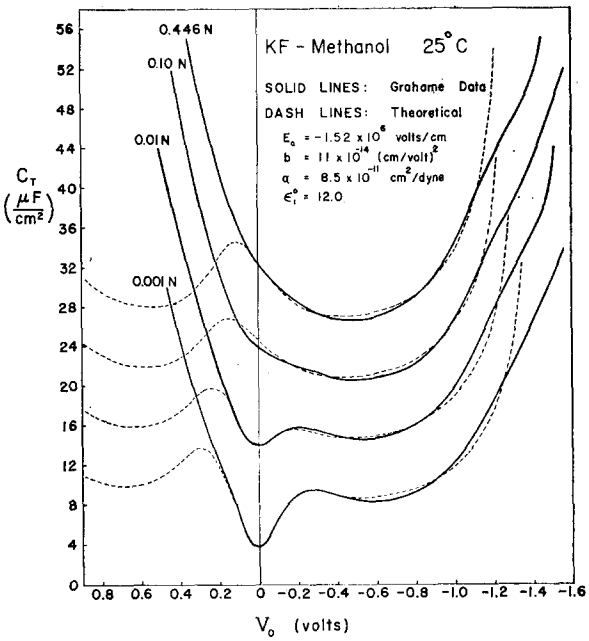


FIG. 11. Comparison of theory and experiment for KF-methanol at 25°C.

and in the present case is likely to be, bigger than the ratio of bulk compressibilities.

The value of $\alpha$ used in Fig. 11 still seems higher than it should be, however, since it leads, in the very approximate fashion discussed earlier, to an actual methanol molecule compressibility somewhat exceeding that of bulk methanol. It may be that some of the final cathodic rise of the curves of Fig. 11 stems from other causes than compression and electrostriction. Minc and Jastrzebska[108] have found considerable dependence of this rising region in methanol solvent on cation species, with $K^+$ giving the largest effect. It is possible, as suggested by these authors, that this ion is specifically adsorbed in this region, and that therefore its contribution to the capacitance should be removed before fitting with compression and electrostriction effects. Such removal would, of course, result in a lower value of $\alpha$.

Cation adsorption, if present, is certainly of more importance for methanol than for water solvent, but it still may have some effect on the high cathodic polarization portion of the water-solvent curves. We believe that specific adsorption of cations and possible water-substitution effects[22o] are sufficient to explain the large magnitude of $\alpha$ found for methanol and the deviations which occur at high cathodic polarization between theory and experiment. Were data available for which the above effects had been or could be eliminated, it might also turn out that the remaining compression and electrostriction processes would be best represented with a value of $m$ greater than the unity value used in Fig. 11. With the value of $\alpha$ used, maximum theoretical $P_E$ is about 4000 atm and maximum inner layer compression is about 30%. At least the last value would certainly be reduced if the true value of $\alpha$ were smaller, as is likely.

Grahame[3] has explained the anodic hump found with NaF in water solvent as arising from the increase in thickness of an ice-like layer next to the electrode as the temperature is lowered. Apparently, the thickness of this layer must be assumed to vary with electrode charge as well, being greater for anodic than for cathodic polarization. Since the hump does not appear in methanol at 25°C, Grahame assumes that there is no solid-like layer for this solvent. In the present theory, a variable-thickness ice-like layer need not be introduced. The hump finds a more natural explanation, we feel, in the interplay between dielectric saturation, including the saturating effect of anisotropic solvent-molecule adsorption, and specific adsorption of anions. The inner layer considered here is not ice-like in its structure since a hexagonally close-packed monolayer cannot approximate to the three-dimensional tetragonal structure of ice. On the other hand, like ice, the monolayer, whether made up of water or methanol, is assumed to have some rigidity. Note that even were the inner region several monolayers of water thick and approximated bulk behavior, the pressure in it would not be sufficient to produce ice VI or VII at 25°C, where traces of the hump still remain for NaF in aqueous solution.

It is believed that the present work is applicable to all differential capacitance measurements with ideal polarized electrodes in polarization regions where no specific adsorption occurs. Fitting of theory to experiment in such cases allows solvent dielectric saturation and electrostriction effects to be separated and quantified, probably the only technique for which this is possible in high field-strength regions. Since the measurements are essentially quasi-static, uncertain dispersion and adiabatic heating effects which may trouble the interpretation of results of pulse methods of dielectric saturation[73] are entirely absent. It also appears that at least crude determination may be made of the compressibility of individual solvent molecules. Finally, the present theory may serve as background for a more complete theory of the double layer which includes a quantitative treatment of specific adsorption.

## ACKNOWLEDGMENTS

The authors have benefited greatly from many discussions with Dr. Robert Stratton. One of the authors (JRM) is greatly indebted to the late Professor David Grahame for stimulating correspondence over a period of several years, without which this paper would not have been written.

[108] S. Minc and J. Jastrzebska, J. Electrochem. Soc. **107**, 135 (1960).